catalysts

MDPI

Review

Propane Oxidative Dehydrogenation on Vanadium-Based Catalysts under Oxygen-Free Atmospheres

Samira Rostom and Hugo de Lasa *

Chemical Reactor Engineering Centre, Faculty of Engineering, University of Western Ontario, 1151 Richmond Street, London, ON N6A 5B9, Canada; srostom@uwo.ca

* Correspondence: hdelasa@uwo.ca; Tel.: +1-519-661-2144; Fax: +1-519-850-2931

Received: 20 March 2020; Accepted: 8 April 2020; Published: 10 April 2020

Abstract: Catalytic propane oxidative dehydrogenation (PODH) in the absence of gas phase oxygen is a promising approach for propylene manufacturing. PODH can overcome the issues of over-oxidation, which lower propylene selectivity. PODH has a reduced environmental footprint when compared with conventional oxidative dehydrogenation, which uses molecular oxygen and/or carbon dioxide. This review discusses both the stoichiometry and the thermodynamics of PODH under both oxygen-rich and oxygen-free atmospheres. This article provides a critical review of the promising PODH approach, while also considering vanadium-based catalysts, with lattice oxygen being the only oxygen source. Furthermore, this critical review focuses on the advances that were made in the 2010–2018 period, while considering vanadium-based catalysts, their reaction mechanisms and performances and their postulated kinetics. The resulting kinetic parameters at selected PODH conditions are also addressed.

Keywords: propane oxidative dehydrogenation; propylene; selectivity; vanadium oxide; lattice oxygen; successive injections; CREC Riser Simulator; kinetic modeling; simulation

1. Introduction

Propylene is one of the most important building blocks in the petrochemical industry [1–3]. It is industrially employed to produce polypropylene, which is used extensively to make packaging and labeling, textile products, laboratory equipment, loudspeakers, and automotive components. Propylene is also used for the manufacturing of acrylonitrile, propylene oxide derivatives, and other substances [4,5]. The current global propylene demand is the range of 90 million metric tons (MMT) per year, according to the IHS Chemical World Analysis. It is estimated that this demand will rise up to 130 MMT per year by 2023 [6,7].

The traditional olefin production involves steam cracking, fluid catalytic cracking (FCC), and catalytic dehydrogenation (DH) [1,3,8–10]. Typical feedstocks for ethane steam cracking are LPG (light petroleum gas) and naphtha. These olefin production processes involve homogeneous reactions where the hydrocarbon species are steam cracked into smaller olefins [3]. For FCC, commonly used feedstocks are vacuum gas oil, refinery hydrocarbon residues, and de-asphalted oil, which are converted into light and higher value products, such as gasoline. Cracking processes are endothermic and, thus, consume large amounts of heat. To accomplish this, these processes require reactor designs that can be operated at high temperatures [9]. Additionally, significant undesirable amounts of coke are formed, imposing severe operating constraints with frequent plant shutdowns [1,10,11].

Catalytic dehydrogenation (CDH) is an economical route for upgrading low-cost saturated alkanes, such as ethane and propane, into the more valuable olefin feedstocks (e.g., ethylene, propylene) [12]. Furthermore, and given the recent increase of shale gas availability [13–15], there is a renewed interest in efficient and economical routes to convert alkanes into olefins. One should note that CDH is

thermodynamically limited [3,8,16]. At the present time, CDH is mainly considered for propane and butane dehydrogenation. In this respect, one can list the several industrial scale processes [8,17] for propane dehydrogenation. These include CATOFIN from ABB Lummus, OLEFLEX from UOP, Fluidized Bed Dehydrogenation (FBD) from Snamprogetti, and Steam Active Reforming (STAR) from Phillips Petroleum. These technologies differ with respect to the catalyst type used, the reactor design employed, and the selected operating conditions. These processes include a dehydrogenation section and a catalyst regeneration section [18,19]. However, CDH displays similar constraints as steam cracking and FCC, with these being, as follows: a) they involve endothermic reactions and b) they require operating temperatures in the 450–700 °C range. At these high temperatures, cracking and coking can occur, which limits the use of potentially valuable catalysts, such as Cr_2O_3/Al_2O_3 and $Pt/Sn/Al_2O_3$. Existing processes are insufficient to satisfy increasing olefin market demands due to these issues, and given that in catalytic cracking (FCC) olefins are only by-products [8,14].

Thus, and to alleviate the issues associated with the dehydrogenation process, oxygen can be added to the reaction medium, promoting ODH (oxidative dehydrogenation) [2]. As a result, the reaction becomes an exothermic and irreversible reaction, overcoming the thermodynamic limitations of dehydrogenation (DH) [5,8,20,21]. Here, water is formed as a stable product. ODH displays large and positive equilibrium constants, with these equilibrium constants decreasing at higher temperatures. Furthermore, the presence of oxygen limits coking and, therefore, extends catalyst usage. It is, in fact, at the 650 °C thermal level where ODH appears to provide a unique opportunity versus thermal or non-oxidative catalytic dehydrogenation (CDH) [9].

Most ODH reactions are carried out in the presence of gaseous oxygen between 400 and 700 °C [22–25]. Catalytic ODH with gas phase oxygen faces challenges, given that it requires one to: (i) co-feed gaseous oxygen and alkanes with this leading eventually to an operation within the explosion region; and, (ii) use an oxygen that is costly and energy intensive to produce and which is manufactured via cryogenic air separation. Furthermore, ODH in the presence of gaseous oxygen may promote the production of electrophilic surface oxygen species such as O^- and O^{2-}, formed via adsorbed gaseous oxygen. This might limit the ODH reaction selectivity [26–29]. Additionally, undesired CO_x might also be formed either by direct alkane combustion or by deep oxidation of the product olefins, reducing olefin selectivity [29,30]. This deep oxidation is facilitated by the different types of bonds, as follows: (a) C–C bonds in alkanes involve sigma bonds with a 347 kJ/mol energy and C–H bonds with 308–435 kJ/mol, (b) C=C in alkenes contains both sigma and pi bonds, with the pi bonds having a much lower 264 kJ/mol bond energy. This helps alkenes to rapidly combust [8,31–33].

Other than CO_x formation, H_2 is a comparatively important product in ODH [20,34]. Non-oxidative dehydrogenation becomes thermodynamically favored at 650 °C and above, with hydrogen formation yielding coke and free radicals [34,35]. In this respect, when O_2 is near depletion, non-oxidative processes dominate the ODH, with the CO_2 and H_2O formed also being consumed. These conditions enhance the overall H_2 yields [36].

Regarding homogeneous gas phase reactions with respect to the light alkane ODH selectivity, it has been shown that they can be of significance above 600 °C [15,20,36–38]. These reactions are initiated at the catalyst surface via C−H bond splitting, with the formation of radicals. These radicals may subsequently be converted into CO_2 in the gas phase [39], which leads to local hot spots and gas phase ethylene combustion losses.

On the other hand, the oxidative dehydrogenation of light alkanes does not have many of the disadvantages of the endothermic pyrolytic processing of hydrocarbons, such as: (a) a high energy consumption, (b) the production of coke, and (c) the formation of a considerable amount of by-products [2]. Major challenges in the implementation of the oxidative dehydrogenation of light alkanes at the pilot and demonstration scale remain, however, the following: (i) the removal of the heat of reaction, (ii) the control of consecutive oxidation reactions. A lack of control leads to the formation of undesirable by-products [29,40,41], and (iii) the keeping paraffin and oxygen mixtures under explosive limits, preventing reaction run-aways [2,42].

While gas phase molecular oxygen might oxidize the deposited carbon on the catalyst surface, it also decreases olefin selectivity via deep oxidation to CO_x. As a result, and due to these various issues, alternative processes that convert paraffins more efficiently in the absence of gaseous oxygen, are highly desirable [13]. The use of mild oxidants has also been proposed to avoid the total oxidation of alkanes [43–48]. To address this issue, mild oxidants, such as nitrogen oxides, are being considered. These mild oxidants still lead to a significant deep alkane oxidation. Another possible mild oxidant is carbon dioxide. CO_2 has been used as a soft oxidant for the ODH of various alkanes (ethane, propane) [15,30,44,49,50], ethylbenzene [51], and methane coupling for ethene production [44]. CO_2 is used due to its advantages in controlling the exothermicity of the reaction [52] and its role as a chemical species diluent. Furthermore, CO_2 offers equilibrium conditions, improving ethylene selectivity, reducing coke formation, and maintaining longer catalyst life. Therefore, utilizing CO_2 is attractive and promising, as CO_2 can be used for the synthesis of valuable products rather than being released it into the atmosphere [44,53]. However, the use of CO_2 suffers from its inherent inertness with a Gibbs Energy of Formation of −394.4 kJ/mol [30]. It is anticipated that the application of a suitable catalyst instead could help to overcome the unfavorable thermodynamics and kinetics of the CO_2 activation barrier. In this respect, the activation of a CO_2 molecule is a foremost challenge for CO_2 utilization in ODH [30].

Several researchers [3,9,10,12,54–59] have studied ethane and propane ODH under oxygen-free atmospheres. These researchers [12,59–63] have investigated light alkane ODH with the only source of oxygen being the catalyst lattice oxygen. ODH via catalyst lattice oxygen prevents deep oxidation, limiting CO_x, and leading to higher olefin selectivity.

Given these interesting prospects, nowadays, ODH under an oxygen-free atmosphere is focused on: (a) the development of new and stable ODH catalysts providing lattice oxygen at low temperatures (e.g., 400–550 °C) and producing very limited carbon oxides, (b) taking full advantage of the favorable thermodynamics, facilitating temperature reactor control [2,8,64–68].

2. Propane Dehydrogenation (DH) and Oxidative Dehydrogenation (PODH) Reactions: Stoichiometry and Thermodynamics

At chemical equilibrium, a reacting system achieves a condition where the total Gibbs Free Energy is minimized [69]. Two approaches are possible for assessing chemical equilibrium: (a) stoichiometric and (b) non-stoichiometric [70,71]. The "stoichiometric" approach requires a defined stoichiometry, involving all reactants and products with their molecular formulae. This stoichiometric approach is the one considered for PODH.

Table 1 reports both the ΔG_R and the ΔH_R, at the reference condition of 298K, for the various reactions that are involved in propane ODH, under both O_2-rich and O_2-free atmospheres. Thus, one can observe that the PODH reactions with gaseous oxygen are more exothermic than the catalytic PODH reactions using the lattice oxygen. Thus, there is in principle, a valuable strategy if PODH reactions are driven by lattice oxygen. These based lattice oxygen reactions can likely provide conditions for the better management of temperature runaways and better control of undesired reactions.

Propane can be converted under the absence of oxygen in the gas phase (e.g., cracking and dehydrogenation relations), as described in Equations (5)–(9). However, these reactions are negligible in the 500–550 °C range and under short reaction times (<20 s). Thus, one can ignore them in equilibrium calculations [59].

However, and if oxygen is co-fed with propane, several reactions can take place as described in Equations (10)–(19). If one examines the negative ΔG_{R298} for all these reactions, one can observe that chemical equilibrium favors various postulated reactions. The equilibrium constant K_r for each of these reactions can be related to the ΔG_r, according to the following equation:

$$K_r = \exp\left[-\frac{\Delta G_r}{RT}\right] \quad (1)$$

where, R is the universal gas constant with a 8.314 J/(mol K) value.

As an example, when considering Equation (10), at 550 °C and with pressures close to atmospheric, one can see that the activities of the chemical species involved in oxy-dehydrogenation can be approximated with their respective partial pressures, as follows:

$$K_r = \frac{P_{C_3H_6} P_{H_2O}}{P_{C_3H_8} P_{O_2}^{\frac{1}{2}}} \quad (2)$$

Chemical species partial pressures can be further expressed in terms of the system total pressure P and the gases mole fractions, as follows:

$$K_r = \frac{[y_{C3H6}][y_{H2O}]}{[y_{C3H8}][y_{O2}]^{\frac{1}{2}}} P^{0.5} \quad (3)$$

In the case of Equation (10) in Table 1, and given that all the other K_{823} equilibrium constants for oxy-dehydrogenation with oxygen being co-fed (Equations (11)–(19) in Table 1) exceed the value of 1 by far, one can see that these gas phase reactions are not limited by chemical equilibrium. The anticipated product molar fractions for gas phase PODH led to limited propylene selectivity with significant yields of the undesirable CO_2 and ethylene [29,30].

Thus, given these facts, the discovery of alternative catalytic pathways for PODH to improve the homogenous PODH is a requirement. One possible promising avenue is the one of using V_2O_5 supported on γ-alumina.

One can see that the PODH, as shown in Table 1 for a V_2O_5 catalyst, might occur via a network of possible reactions (Equations (20)–(24)). For Equation (20) of Table 1, the following relation is anticipated under chemical equilibrium:

$$K_r = \frac{[y_{C3H6}][y_{H2O}]}{[y_{C3H8}]} P \quad (4)$$

Equation (20) (refer to Table 1) displays a $\Delta G_{R,298} = -41.5$ KJ/mol and a $K_{823K} = 5.88 \times 10^8$, as reported in Figure 1. This shows that the PODH is unconstrained by chemical equilibrium at the anticipated selected process conditions. While this is favorable, one can also see that there is a host of other undesirable secondary reactions with even larger $\Delta G_{R,298}$ competing with Equation (20).

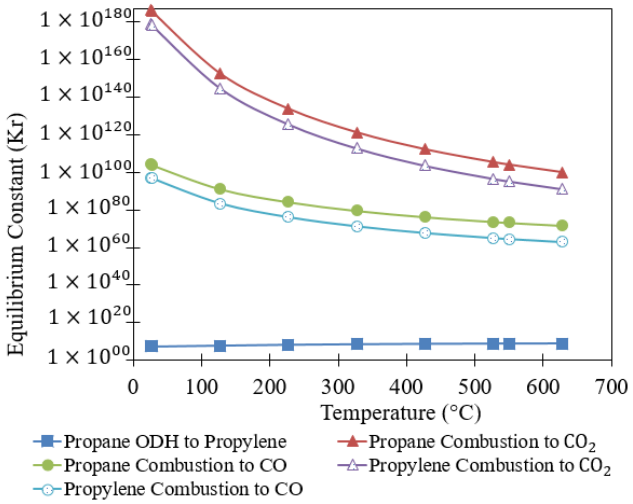

Figure 1. Chemical Equilibrium Constants as a Function of Temperature for Propane ODH under an O_2-free Atmosphere. Total pressure: 1 atm.

Thus, thermodynamic equilibrium analysis for catalytic PODH oxy-dehydrogenation is valuable. It shows the promise of PODH via Equation (20) while pointing to the need of new catalysts to achieve high propylene selectivities.

Finally, and regarding the ODH process under an O_2-free atmosphere, the catalyst regeneration reaction ($2V_2O_4 + O_2 = 2V_2O_5$), which can be calculated by Equation (25) in Table 1, can be effected in a separate regenerator unit. This catalyst regeneration is both spontaneous and exothermic. Therefore, the energy for the PODH under an O_2-free atmosphere with a high selectivity for propylene being endothermic can be recovered from the catalyst regeneration reaction.

Table 1. Gibbs Free Energy and Enthalpy Changes for Propane Dehydrogenation (DH) and Oxidative Dehydrogenation (ODH) Reactions.

Possible Reactions	Chemical Reactions		$\Delta G^0_{f(298)}[\frac{kJ}{mol}]$	$K_{(823K)}$	$\Delta H^0_{f(298)}[\frac{kJ}{mol}]$
Dehydrogenation (DH) [72]	$C_3H_8\ (g) \leftrightarrow C_3H_6(g) + H_2(g)$	(5)	86.2	1.11×10^{-1}	124.3
	$C_3H_8(g) \rightarrow CH_4(g) + C_2H_4(g)$	(6)	41.0	7.47×10^{1}	81.4
	$C_2H_4(g) + H_2(g) \rightarrow C_2H_6(g)$	(7)	−101.3	1.31×10^{2}	−137.2
	$C_3H_8(g) + H_2(g) \rightarrow CH_4(g) + C_2H_6(g)$	(8)	−60.2	9.80×10^{3}	−55.7
	$C_3H_8(g) = 3C\ (s) + 4H_2(g)$	(9)	23.4	3.69×10^{8}	103.9
O_2-Rich Atmosphere [5,8,68,72,73]	$C_3H_8(g) + 0.5O_2(g) \rightarrow C_3H_6(g) + H_2O\ (g)$	(10)	−142.4	7.72×10^{11}	−117.6
	$C_3H_8(g) + 5O_2(g) \rightarrow 3CO_2(g) + 4H_2O\ (g)$	(11)	−2074.2	1.83×10^{135}	−2044.0
	$C_3H_8(g) + 3.5O_2(g) \rightarrow 3CO(g) + 4H_2O(g)$	(12)	−1302.7	1.20×10^{95}	−1195.1
	$C_3H_6(g) + 4.5O_2(g) \rightarrow 3CO_2(g) + 3H_2O(g)$	(13)	−1931.8	2.62×10^{122}	−1926.4
	$C_3H_6(g) + 3O_2(g) \rightarrow 3CO(g) + 3H_2O(g)$	(14)	−1160.2	1.56×10^{83}	−1077.5
	$CO\ (g) + 0.5O_2(g) \rightarrow CO_2(g)$	(15)	−257.2	2.47×10^{13}	−283.0
	$C_3H_8(g) + 1.5O_2(g) \rightarrow C_2H_4(g) + CO(g) + 2H_2O(g)$	(16)	−502.6	1.99×10^{39}	−437.9
	$C_3H_8(g) + 2O_2(g) \rightarrow C_2H_4(g) + CO_2(g) + 2H_2O(g)$	(17)	−759.8	4.93×10^{52}	−720.8
	$C_3H_6(g) + O_2(g) \rightarrow C_2H_4(g) + CO(g) + H_2O(g)$	(18)	−360.2	2.58×10^{27}	−320.3
	$C_3H_6(g) + 1.5O_2(g) \rightarrow C_2H_4(g) + CO_2(g) + H_2O(g)$	(19)	−617.4	6.39×10^{40}	−603.3
O_2-Free Atmosphere [10,12]	$C_3H_8(g) + V_2O_5(s) = V_2O_4(s) + C_3H_6(g) + H_2O(g)$	(20)	−41.5	5.88×10^{8}	5.9
	$C_3H_8(g) + 10V_2O_5(s) = 10V_2O_4(s) + 3CO_2(g) + 4H_2O(g)$	(21)	−1065.2	1.20×10^{104}	−809.7
	$C_3H_8(g) + 7V_2O_5(s) = 7V_2O_4(s) + 3CO(g) + 4H_2O(g)$	(22)	−596.3	1.79×10^{73}	−331.1
	$C_3H_6(g) + 9V_2O_5(s) = 9V_2O_4(s) + 3CO_2(g) + 3H_2O(g)$	(23)	−1023.6	2.04×10^{95}	−815.6
	$C_3H_6(g) + 6V_2O_5(s) = 6V_2O_4(s) + 3CO(g) + 3H_2O(g)$	(24)	−554.8	3.05×10^{64}	−337.0
Catalyst Regeneration [10]	$2V_2O_4(s) + O_2(g) \rightarrow 2V_2O_5(s)$	(25)	−201.8	1.72×10^{6}	−246.9

3. Conversion, Selectivity and Yield Calculations

Paraffin conversion in PODH can be described while using two possible approaches, as described in Table 2:

(a) Propane conversion based on Equation (26), using as the basis, the propane fed to the reactor unit. This equation might involve inaccuracies given the potential gas leaks throughout the reactor unit [3,9,56,74–76].

(b) Propane conversion calculated via Equation (27). This propane conversion provides a more accurate propane conversion than Equation (26), as it is dependent on the outlet product measured while using the outlet FID products [10,12,77,78].

Furthermore, propylene selectivity is also a very important reaction parameter. It is subject to similar potential errors than propane conversion, given it is based on input feed conditions (Equation (28)) [3,76]. As an alternative, Equation (29) provides, in principle, a more adequate selectivity definition, where all products need to be considered, including water [9,56,75]. The use of Equation (29) is frequently not recommended, given that water measurements offers analytical challenges and is often inaccurate. As an alternative, Equation (30) using carbon containing species established using output product FID analysis [10,12,74,77,78] excluding water is strongly recommended. Furthermore,

and regarding product yields, Equation (31) accounts for the product between propane conversion and propylene selectivity [12,75–78]. Consequently, this equation relies on the accuracy of the calculated conversion and selectivity.

Therefore, Equations (27), (30), and (31) are recommended for the calculations of the conversion, selectivity, and yields of propane, respectively.

Table 2. Propane Conversion, Propylene Selectivity, and Propylene Yield Calculations.

Conversion		
$X_{C3H8} = \frac{n_{C3H8,\ in} - n_{C3H8,out}}{n_{C3H8,\ in}} \times 100\%$	(26)	where, $n_{C3H8,in}$ = moles of propane in; $n_{C3H8,out}$ = moles of propane out; ν_i = number of carbon atoms in gaseous carbon containing product i; n_i = moles of gaseous carbon containing product i.
$X_{C3H8} = \frac{\sum_i \nu_i n_i}{3n_{C3H8,\ out} + \sum_i \nu_i n_i} \times 100\%$	(27)	
Selectivity		
$S_i = \frac{n_{ii}}{n_{C3H8,\ in} - n_{C3H8,out}} \times 100\%$	(28)	where, n_{ii} = moles of product i; n_T = total products moles.
$S_i = \frac{n_{ii}}{n_T - n_{ii}} \times 100\%$	(29)	
$S_i = \frac{\nu_i n_i}{\sum_i \nu_i n_i} \times 100$	(30)	
Yield		
$Y_{C3H6} = \frac{X_{C3H8}\ (\%) \times S_{C3H6}(\%)}{100}$	(31)	

4. Vanadium-Based Alkane ODH Catalysts

Catalyst development for ODH reactions has focused on a variety of metal oxides alone or combined with additives (alkali metals and halides). These oxides can be deposited on a variety of supports. While the first studies used metal oxides as catalysts directly, supported catalysts show advantages over unsupported catalysts [79], as follows: a) they provide a better control of metal loading and metal dispersion, and b) they offer an added flexibility to adjust physicochemical properties. For example, TiO_2 supported $VOPO_4$ catalysts give higher ethylene selectivity than the unsupported VO_x and $(VO)_2P_2O_7$ catalysts [80]. Furthermore, researchers [28,50] also focused on promoter addition, which can be used to improve the catalyst performance. Promoters isolate active surface species, forming secondary metal oxides on the support surface.

Research on catalysts for the ODH process usually falls into two operating thermal levels: above or below the temperatures at which significant gas phase reactions take place. High temperature catalysts mainly contain alkali-metal and/or alkaline-earth-metal oxides supported on transition-metal oxides, rare-earth-metal oxides, and other catalytic materials. Low temperature catalysts, on the other hand, usually consist of reducible transition metal oxides [12,59].

As alkali and alkaline earth-based catalysts contain non-reducible ions and oxides, temperatures in excess of 600 °C are needed for adequate ODH reactivity. However, higher reaction temperatures are less favorable for high olefin selectivity. Therefore, reducible transitional metal oxide catalysts are considered instead. This catalyst group can activate the paraffins at low temperatures. However, while catalytic activity is usually higher with this class of catalysts, lower alkene selectivities are frequently found. The oxides of these metals contain removable oxygen (lattice oxygen), which participates in the ODH reactions under oxygen-free atmosphere conditions. However, lattice oxygen is also involved in the un-selective pathways of ODH, forming carbon oxides. Therefore, different catalyst groups can be studied to find the optimum catalyst that will provide high selectivity of olefins [10,12,27,54,55,59,63,81].

Vanadium is the most frequently considered element for ethane and propane ODH. In particular, the VO_x shows promising results for olefin production under an oxygen-free environment [12,54,59,61]. VO_x has a suitable atomic geometry and electronic structure. Furthermore, the V^{4+} and V^{5+} valence states make vanadium valuable for many catalytic reactions [82]. Moreover, supported vanadium oxides have attracted significant attention due to their higher performances, better thermal stabilities, and large specific surface areas.

In this respect, the stoichiometric equation for the conversion of propane ODH to propylene over vanadium-based catalysts is as follows:

$$C_3H_8 + MO_x \rightarrow C_3H_6 + H_2O + MO_{x-1} \quad (32)$$

This reduced vanadium species is regenerated via molecular oxygen following the stoichiometry described below:

$$MO_{x-1} + \frac{1}{2}O_2(\text{air}) \rightarrow MO_x \quad (33)$$

The redox behavior of supported vanadia catalysts in ODH is generally controlled by three main factors: (i) the VO_x surface structure; (ii) the acid-base character of the metal and the support; and, (iii) the redox properties of the VO_x species. These three properties are influenced by the support type and vanadium loading [83,84].

4.1. VO_x Surface Coverage

The molecular structures of surface vanadia species on metal oxide supports have been reported in the technical literature [85–88]. These studies suggest that, depending on the vanadium loading on the support, four kinds of VO_x surface species can be present on the catalyst surface: (a) isolated VO_4 species (monovanadate); (b) polymeric VO_4 species (polyvanadates); (c) a mix of both isolated and polymeric VO_4 surface species; and, (d) V_2O_5 crystals. Some studies [83,88–91] showed that, at low vanadium loading, a highly dispersed isolated VO_4 surface species (monovanadates) is formed. As the VO_x surface density increases with vanadium loading, the surface configuration evolves from isolated monovanadates to polymeric polyvanadates. In this respect, it appears that polymeric polyvanadate dominates until a vanadia monolayer surface coverage is reached. However, at high vanadium loadings, crystalline V_2O_5 nanoparticles form on top of the vanadia monolayer. It is generally accepted that isolated tetrahedral VO_x species (which are obtained at low vanadium loading) are more ODH selective but less active than polymeric VO_x species [88–90].

4.2. Active Lattice Oxygen Species

Other than the ODH catalyst structure, the binding strength of the surface lattice oxygen in the VO_x surface species is a main parameter that governs the activities and selectivities of alumina-supported vanadia catalysts. In extensive structural studies [87,92,93] of supported vanadium oxide catalysts, three types of lattice oxygen bonds were identified (Figure 2): (a) terminal V=O bonds, (b) bridging V–O–V bonds, and (c) V–O–support bonds. Each type of lattice oxygen has a different binding strength. The studies were aimed at determining which type of lattice oxygen bond is responsible for the oxidation activity, which occurs in various catalytic oxidation reactions [92,94]. It was determined that the oxygen in the V–O-support bond, rather than the terminal V=O or the V–O–V bonds, is the one that is involved in this catalytic oxidation reaction.

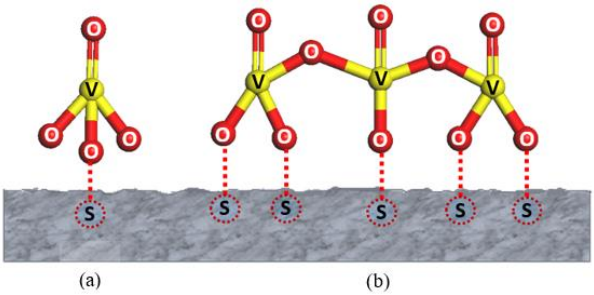

Figure 2. (**a**) Isolated VO_4 species on the support (s); and, (**b**) Polymeric VO_4 species on the support (s).

4.3. Effect of Support (Acid/Base Properties)

Metal oxides are composed of redox metal cations and lattice oxygen anions. These are Lewis acid and basic sites, respectively. Thus, the acid-base support characteristics may contribute with several effects, namely:

(a) the dispersion of the active species;
(b) the specific structure of the active species;
(c) the reactant molecule activation;
(d) the rates of competitive pathways of transformation; and,
(e) the rates of adsorption and desorption of reactants and products.

Furthermore, the acid-base support can influence the vanadium-based catalyst reactivity or olefin selectivity [83,93–96]. For instance, the interaction between the acidic V_2O_5 species and a basic support might be strong (e.g., MgO, La_2O_3, Sm_2O_3). This might lead to the formation of highly dispersed VO_x species, which is responsible for the high alkene selectivities. In contrast, the interaction between the acidic V_2O_5 and an acidic support (e.g., SiO_2, Al_2O_3) may be weak. This might lead to a less dispersed vanadium species, which favors the formation of a less active V_2O_5 crystalline phase [95,97,98].

Moreover, on acidic catalysts, basic reactant adsorption and acidic product desorption are favored. Thereby, this protects the chemical species from further oxidation to carbon oxides. For instance, higher selectivities to ethylene have been obtained using acidic based catalysts, like the VO_x/γ-Al_2O_3 catalysts. These findings were justified, given that higher support acidity decreases the interaction between the ethylene product and the catalyst [55,97]. In addition, dominant Brønsted acid sites are considered to be desirable to facilitate rapid olefin desorption and limit the complete alkane oxidation to CO_x. Thus, catalyst acidity and acid site type have to be kept at acceptable levels. This is required, so as to not interfere with the overall catalyst activity and catalyst olefin selectivity [96].

4.4. Redox Properties of Supported VO_x Catalysts

The reducibility of vanadium oxides is considered to be one of the main factors influencing their activity in partial oxidation reactions and, in particular, in the ODH reactions of alkanes. There is, in fact, a close relationship between catalyst reducibility and VO_x surface structure on a given metal oxide support. In this respect, the reducibility of the surface VO_x species increases with surface VO_x coverage. Thus, the following trend for the reducibility of the different supported vanadia species can be considered as follows: polymeric surface VO_x > isolated surface VO_x > crystalline V_2O_5 nanoparticles [83,96,99]. Moreover, the type of support used affects the extent of the reducibility of supported vanadium oxide catalysts.

The catalyst support acid-base character also affects redox properties. One can observe that there is decreasing reducibility of the vanadium species when using more basic support oxides [100]. Moreover, the propane ODH reaction runs conducted at 450–550 °C showed the following: (a) the V_2O_5/TiO_2 catalyst, which is less basic and easier to reduce, is the most active catalyst, (b) the V_2O_5/Al_2O_3 catalyst, which is more acidic and difficult to reduce, is the most selective in propylene production. These

variations of vanadia oxide reducibilities on different metal oxide supports could be related to the different reducibilities of the various V–O–support bonds existing on different support types [83,97,100].

Thus, one can conclude that the catalytic activities and selectivities of the supported vanadium oxide catalysts are significantly affected by the properties of the support oxide material, the interaction of the surface VO_x species with the oxide support, and the vanadium loading. The redox sites are in charge of transferring the lattice oxygen to the adsorbed propane to form propylene. The acid sites catalyze the condensation of the intermediates. Therefore, it is necessary to investigate the synergistic effects of the redox and acidic properties of a catalyst as well as their dependence on the catalyst composition and reaction conditions to enhance the efficiency of such a process.

4.5. Propane ODH Catalysts

To date, several vanadium-based catalysts have been studied for PODH. In these cases, the only oxygen source was the catalyst lattice oxygen. This research has been led in the last few years by Prof. de Lasa's research team at the Chemical Reactor Engineering Centre (CREC), University of Western Ontario Canada [12,55,101,102].

Rostom et al. [59,60] established a mixture of ZrO_2 and γAl_2O_3 (1:1 weight ratio) as a support for a vanadium-based catalyst. These authors loaded different percentages of vanadium (5, 7.5, and 10 wt. % V) on this support and achieved the best result with 7.5 wt. % vanadium loading. So far, this is the best-reported propane conversion (25%) and propylene selectivity (94%) combination with a negligible amount of CO_x selectivity (2.1%) at 550 °C. The same support was utilized by researchers [54,56,75] for ethane ODH in the temperature range of 525–600 °C and with 20–50 s contact times. They achieved 82% ethylene selectivity at 8.5% ethane conversion.

Hossain et al. [10,61] developed a vanadium-based CaO-γAl_2O_3 support for propane ODH. They prepared CaO to γAl_2O_3 weight ratios of 1:4 and 1:1 and achieved the best results with the 1:1 weight ratio. They performed ODH at a 550–640 °C temperature range and achieved 25.5% propane conversion, 94.2% propylene selectivity, and 5.8% CO_x selectivity at 640 °C. This high temperature had a negative impact on the ODH reaction.

Ghamdi et al. [12] reported different PODH catalysts prepared with various vanadium loadings on γAl_2O_3 (5, 7, and 10 wt. % V) for propane ODH at 475–550 °C and reaction times of 5–20 sec. The re-adsorption of the propylene product was assigned to methane, ethane, and ethylene cracking, as γ-Al_2O_3 is acidic in character. Therefore, the maximum selectivity of propylene that these authors achieved was 85.94% at 11.73% propane conversion. The rest of the products were CO_x, CH_4, C_2H_4, and C_2H_6.

Fukudome et al. [62,63] incorporated VO_x species into a SiO_2-frame to obtain a higher concentration of isolated VO_x species. This catalyst was synthesized by an alkoxy exchange between a metal alkoxide and polyethylene glycol. Following this, PODH using a VO_x lattice oxygen was performed in a fixed-bed reactor at a 450 °C temperature under atmospheric pressure. These researchers found that VO_x that was incorporated into the SiO_2 showed higher propylene selectivity than VO_x loaded onto SiO_2. This could be ascribed to the isolated VO_4^{3-} species in the silica framework.

Table 3 reports the various reaction conditions and experimental results when using vanadium-based catalysts on different supports, where catalysts lattice oxygen is the only oxygen source.

Table 3. Propane ODH catalysts.

ODHP Catalyst	Feed	Reactor	Method	T (°C)	Reaction Time	X_{C3H8}	Selectivity (%) S_{C3H6}	Selectivity (%) S_{COx}	Y_{C3H6}	Year
7.5 wt.% V/ZrO_2-γAl_2O_3	C_3H_8	Fluidized bed	Successive	550	20 s	25.00	94.00	2.10	23.50	2017 [59]
7.5 wt.% $V/\gamma Al_2O_3$	C_3H_8	Fluidized bed	Successive	550	20 s	25.70	89.30	3.70	22.90	2017 [59]
VO_x/CaO-γAl_2O_3	C_3H_8	Fluidized bed	Successive	550–640	10–31 s	10.30–25.50	78.30–94.20	5.80–21.70	8.10–24.00	2017 [61]
5% $VO_x/\gamma Al_2O_3$	C_3H_8	Fluidized bed	Successive	475–550	5–20 s	2.35–11.73	70.89–85.94	86.49–96.90	2.76–5.41	2014 [12]
7% $VO_x/\gamma Al_2O_3$	C_3H_8	Fluidized bed	Successive	475–550	5–20 s	3.24–13.36	60.73–75.34	10.43–35.81	2.57–7.21	2014 [12]
10% $VO_x/\gamma Al_2O_3$	C_3H_8	Fluidized bed	Successive	475–550	5–20 s	3.73–15.05	55.12–67.77	15.01–41.52	2.48–8.72	2014 [12]
V(1.0)-PEG25	C_3H_8	Fixed-bed	Single	450	8 min	2.00	94.80	1.90	1.90	2013 [62]
VO_x/SiO_2	C_3H_8	Fixed-bed	Single	450	8 min	3.00	88.30	7.00	23.90	2011 [63]

5. Experimental Laboratory Reactors for PODH

The CREC Riser Simulator [103,104], as described in Figure 3, is a bench-scale mini-fluidized bed reactor (53 cm^3).

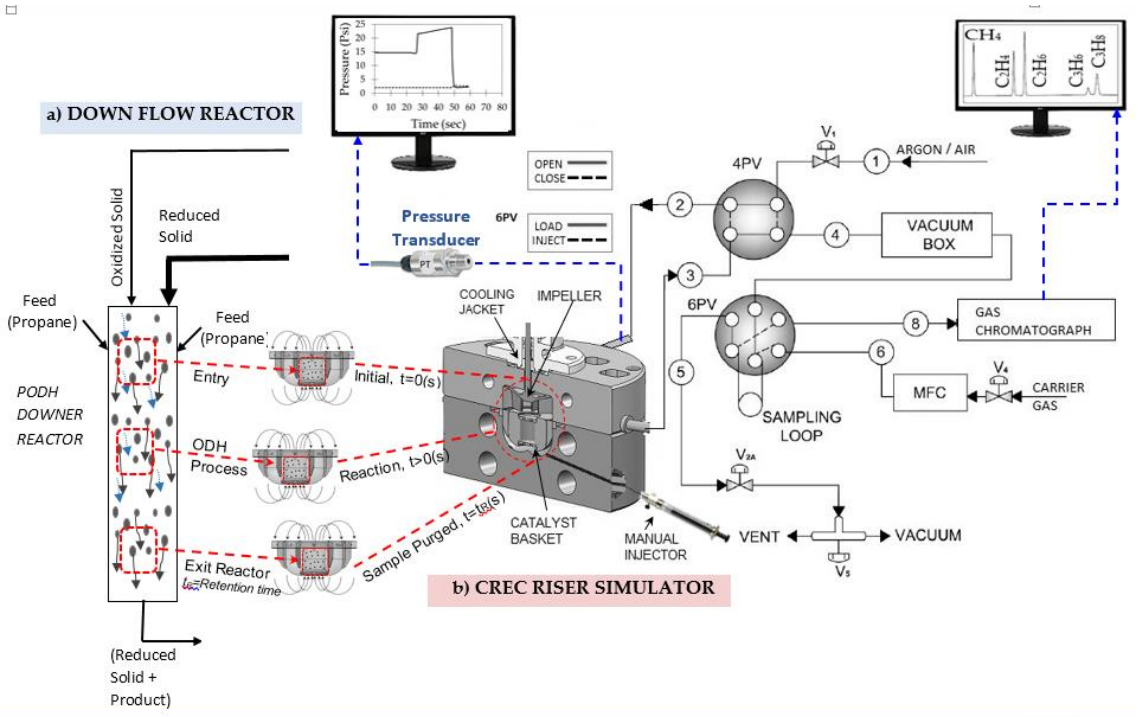

Figure 3. Schematic Diagram Describing: (**a**) A propane oxidative dehydrogenation (PODH) downflow reactor, (**b**) The Chemical Reactor Engineering Centre (CREC) Riser Simulator including the main reactor unit, auxiliary valves, the pressure measurements and the analytical system.

It provides conditions that are equivalent to those of a twin circulating fluidized reactor process (reactor–regenerator). CREC researchers have already demonstrated promising ethane conversions and ethylene selectivities using this reactor. Here, a VO_x/γ-Al_2O_3 catalyst is utilized in the absence of molecular gas oxygen. In the CREC Riser Simulator, VO_x/c-Al_2O_3 [84], VO_x-MoO_x/γ-Al_2O_3 [3], VO_x-Nb/La-γ-Al_2O_3 [9], and VO_x/γ-Al_2O_3-ZrO_2 [54,56,76] catalysts were used for ethane ODH. VO_x/γ-Al_2O_3 [12], VO_x/CaO-γ-Al_2O_3 [10,61], and VO_x/γ-Al_2O_3-ZrO_2 [59,60] catalysts were used in propane ODH in this reactor in the absence of gas phase oxygen. This reactor operates under batch conditions and it is designed for catalyst evaluation and kinetic studies under fluidized bed (riser/downer) reactor conditions. One of the main advantages of this unit is its capability to simulate

fluidized bed reactions conditions by using a very small amount of catalyst. Details of this reactor are found in literature [12].

Figure 4a–c describe typical PODH pressure profiles in the CREC Riser Simulator during and after the reaction. Initially, as propane is being fed via a syringe into the reactor at atmospheric pressure, the reactor pressure increases significantly. Following this, the reactor pressure is further augmented, while the PODH reaction is progressing. Finally, and a preset time, the unreacted feed and the products are transferred almost instantaneously to a vacuum box, with the reactor pressure decreasing abruptly.

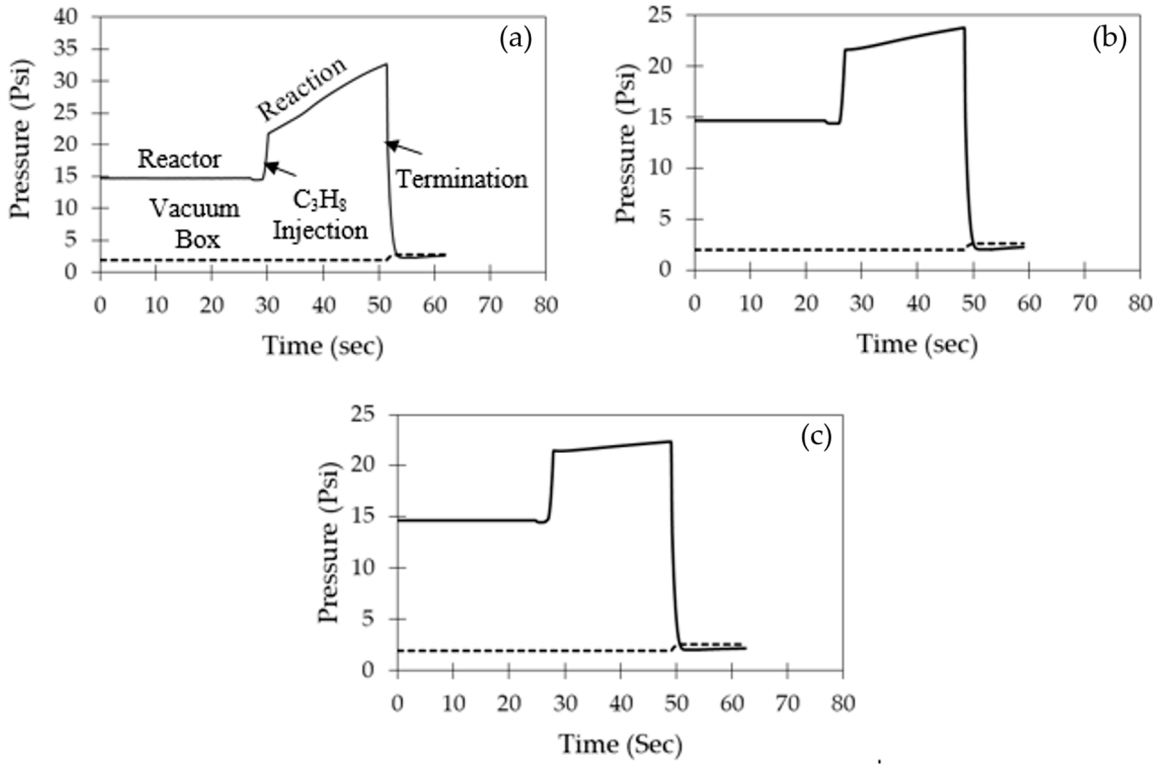

Figure 4. Pressure profile in the CREC Riser Simulator for consecutive propane ODH reaction. (**a**) After 1st injection; (**b**) After 2nd injection; and, (**c**) After 10th injection.

Regarding the studies in the CREC Riser Simulator, two modes of operation were considered: (a) single propane injections with catalyst regeneration in between, and (b) ten consecutive propane injections without catalyst regeneration in between. These types of possible PODH operations are discussed in the upcoming sections.

5.1. Single Propane Injection

A single propane injection in the CREC Riser Simulator allows for one to understand the interaction between the alkane feed and a fully oxidized catalyst. Thus, in these experiments, the catalyst is repeatedly reduced when reacting with the alkane and then re-oxidized by air at various reaction temperatures and contact times. Following every reaction injection, the catalyst is regenerated with air. Therefore, every time the catalyst is regenerated, the PODH is mainly driven by non-selective oxygen species on the catalyst surface. This could involve loosely bound lattice oxygen or weakly adsorbed oxygen species [59,61]. This loosely bound lattice oxygen is considered to be more reactive and, thus, more likely to cause carbon-carbon bond breakage, promoting propane total oxidation. As a result, both types of oxygen species may contribute to the total oxidation of propane and lead to low propylene selectivity. Therefore, it can be concluded that fully oxidized (fresh) catalysts are active, but not selective, in propane ODH reactions [12]. In addition, single injections followed by catalyst re-oxidation show the value of using a catalyst with an optimized oxygen state, where the

density of the oxygen species on the catalyst surface is controlled. This is significant in achieving higher propylene selectivity.

5.2. Successive Propane Injections

Successive propane injections can be implemented to overcome the problem of single injection experiments where low propylene selectivity is an issue, as described in Figure 4a–c. Here, the PODH catalyst is progressively reduced via the consecutive alkane injections and, therefore, propylene selectivity gradually increases. There is, as mentioned, no catalyst regeneration in between propane injections.

With these data and for each of the injections, the instantaneous conversions and selectivities for the main products can be calculated. Furthermore, the degree of reduction of the catalyst can be defined as the ratio of the remaining oxygen in the catalyst after each injection to the original oxygen content of the catalyst. The former can be determined by analyzing the various oxygen-containing products resulting from each alkane injection. The latter can be calculated from the oxygen uptake of the O_2-chemisorption characterization technique.

In this respect, researchers reported high propylene selectivity and good propane conversion while following the second and third successive injection [12,59,61]. This is the case, given that successive injections deplete quickly weakly adsorbed oxygen species. Furthermore, only then, the catalyst lattice oxygen drives the PODH reaction. For instance, a VO_x/ZrO_2-γAl_2O_3 catalyst that was developed at CREC-UWO and used with multiple injections yielded 25% propane conversion with 94% selectivities [60].

Figures 5 and 6 report propane conversion, and propylene and carbon oxide selectivity, respectively, with every injection. Initially, due to the presence of surface oxygen, propane conversion and CO_x selectivity are high with a very low propylene selectivity. After the first injection, surface oxygen decreases and lattice oxygen starts contributing to PODH, as shown in Appendix A. There is a drop in propane conversion and CO_x selectivity, and a rise in propylene selectivity. From the third to the tenth injections, propane conversion, propylene, and CO_x selectivities are almost constant due to the effect of the lattice oxygen.

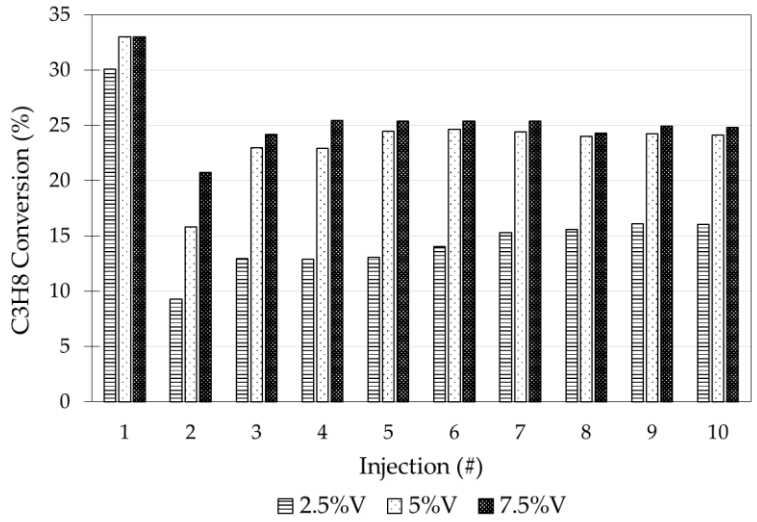

Figure 5. Propane Conversion during Consecutive Oxidative Dehydrogenation (ODH) Cycles over Various (2.5, 5, and 7.5 wt.% V) VO_x/ZrO_2-γAl_2O_3 Catalysts (Operating conditions: T = 550 °C, reaction time = 20 s, C_3H_8 injected = 10 mL, catalyst loaded = 0.76 g). Standard deviations for repeats: 1.5%. Note: Reported values are based on propane conversion into carbon containing gas phase products. Adapted with permission from [59], copyright 2017, American Chemical Society.

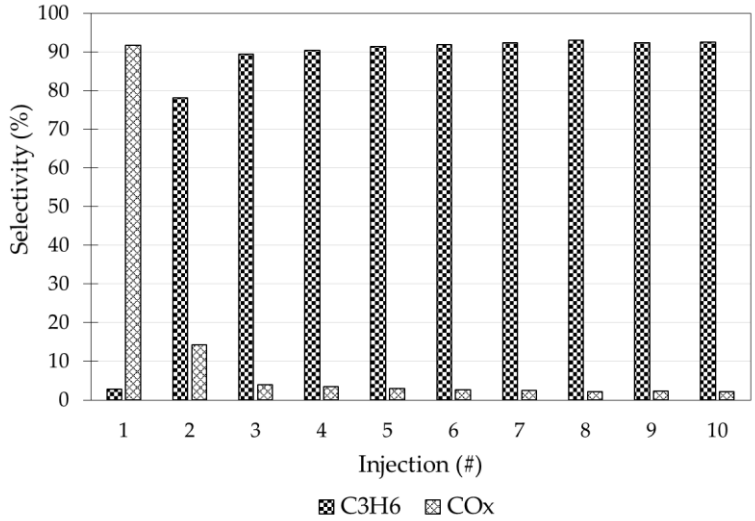

Figure 6. Propylene and CO_x Selectivities during Consecutive ODH Cycles using VO_x/ZrO_2-γAl_2O_3 (7.5 wt.% V) Catalysts (Operating conditions: T = 550 °C, reaction time = 20 s, C_3H_8 injected = 10 mL, catalyst loaded = 0.76 g). Standard deviations for repeats: 1.5%. Note: Reported selectivities are based on propane conversion into carbon containing gas phase products. Adapted with permission from [59], copyright 2017, American Chemical Society.

6. Kinetics and Reaction Mechanisms of Propane ODH over Vanadium-Based Catalysts

Baerns et al. reported [105] the mechanism of the initial activation of the free radicals in the alkane ODH reaction over transition metal oxides (i.e., VO_x, MoO_x etc.). According to this, oxygen from the metal oxide extracts hydrogen from the alkane. The OH groups formed are then removed from the catalyst surface by dehydration. Thus, the catalyst surface is reduced in the formation of propylene and the products of total oxidation (COx). Thus, and as a result, the catalyst has to be subsequently re-oxidized by gas phase oxygen. This type of mechanism is known as the ODH redox-mechanism, as described by Equation (34).

$$C_nH_{2n+2} \overset{MeO_x}{\rightarrow} C_nH_{2n+1} + MeO_xH \rightarrow C_nH_{2n} + MeO_{x-1} + H_2O \overset{\frac{1}{2}O_2}{\rightarrow} C_nH_{2n} + MeO_x + H_2O \quad (34)$$

PODH has been extensively studied using vanadium-based catalysts. This has been done in order to understand the selective pathways for propylene production [101,106–110]. All of these studies revealed that PODH consists of a set of consecutive and parallel reactions: (a) the ODH of propane; (b) the undesired combustion of propane to CO_x; and, (c) the secondary combustion of propylene to CO_x (Figure 7). The two latter reactions can limit the propylene selectivity and the propylene yield during PODH. Furthermore, it is generally agreed that, as propane conversion increases, selectivity towards the desired propylene decreases. Therefore, a significant fraction of the propane and/or propylene is unselectively converted into carbon oxides.

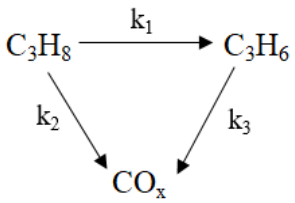

Figure 7. Reaction Network for PODH. Reprinted with permission from [60], copyright 2018, American Chemical Society.

Thus, the major challenge of PODH is to control the propylene selectivity, as the alkenes formed during ODH tend to be combusted via a secondary reaction.

Recent literature has reported the feasibility of the Mars van Krevelen [101,111] and Langmuir Hinshelwood [60,61] mechanisms for gas phase oxygen-free PODH. It was hypothesized that the dominant reaction mechanism for catalytic alkane ODH involves transition metal oxides. The reaction steps include catalyst lattice oxide being reduced by adsorbed alkanes. In this case, olefins are formed through several possible intermediate species. Gas phase molecular oxygen can then re-oxidize the reduced catalyst sites.

Rostom et al. [60] reported the feasibility of the Langmuir–Hinshelwood mechanism for PODH kinetic modeling under oxygen-free conditions. The adsorption constants were independently defined through experiments in the CREC Riser Simulator. These authors found that the high propylene selectivity can be justified given the much larger 2.82×10^{-5} mol.gcat^{-1}s^{-1} frequency factor for propylene formation versus the 1.65×10^{-6} mol.gcat^{-1}s^{-1} frequency factor for propane combustion. However, calculated energies of activation (55.7 kJ/mol for propylene formation and 33.3 kJ/mol for propane combustion) appear to moderate this favorable effect on propylene selectivity, with the influence of frequency factors prevailing. Furthermore, propylene conversion into CO_x oxidation appears as a non-favored reaction step given the 98.5 kJ/mol activation energy and 4.80×10^{-6} mol.gcat^{-1}s^{-1} frequency factor. This kinetic model is considered of special value for the further development of a scaled-up twin fluidized bed reactor configuration for PODH.

Hossain et al. [61] compared the kinetics of the oxidative dehydrogenation (ODH) of propane to those of propylene over VO_x/CaO and VO_x/CaO-γAl_2O_3 catalysts in the absence of gas phase oxygen through the Langmuir−Hinshelwood mechanism. These researchers found that propylene formation using a VO_x/CaO-γAl_2O_3 catalyst has a lower activation energy (120.3 kJ/mol) than the one when using the VO_x/CaO (126.7 kJ/mol) catalyst. In contrast, the VO_x/CaO-γAl_2O_3 catalyst requires higher activation energies (55.2 kJ/mol) than the VO_x/CaO catalyst (32.8 kJ/mol), in order to prevent the undesired CO_2 formation. These values are consistent with the product selectivity, as observed in the catalyst evaluation experiments.

Ghamdi et al. [101] reported the kinetic modeling of propane oxidative dehydrogenation (ODH) via the Mars van Krevelen mechanism. The calculated pre-exponential factors ($k_1{}^0$, $k_2{}^0$, and $k_3{}^0$) increased as the vanadium loading was augmented. In addition, the activation energies for CO_x formation (E_2 and E_3) were consistently smaller than the ones for propylene formation (E_1).

Table 4 displays the activation energy values for propane ODH reactions under gas phase oxygen-free conditions, as reported in the technical literature.

Table 4. Activation Energies and Activity Decay Parameter Values for the Main Products from PODH, as Reported in the Literature.

Catalyst	Activation Energy of Formation (kJ/mol)			Decay Parameter (λ)	Year
	C_3H_6	Carbon Oxides			
7.5 wt.% V/ZrO_2-γAl_2O_3	55.7	(CO_x) 33.3 [a]	(CO_x) 98.5 [a]	0	2018 [60]
10% VO_x/CaO-γAl_2O_3 (1:1)	120.3	(CO_2) 55.1 [a]	(CO_2) 53.7 [b]	$1.6\times10^{-3} \pm 0.6\times10^{-3}$	2017 [61]
5% VO_x/γAl_2O_3	124.92	(CO_x) 52.81 [a]	(CO_x) 52.54 [b]	0.01–0.053	2014 [101]
7% VO_x/γAl_2O_3	115.08	(CO_x) 51.07 [a]	(CO_x) 52.73 [b]	0.017–0.056	2014 [101]
10% VO_x/γAl_2O_3	109.42	(CO_x) 45.58 [a]	(CO_x) 53.75 [b]	0.015–0.047	2014 [101]

[a] Formation from propane; [b] Formation from propylene.

7. Parameters that Affect ODH Reactions

7.1. Effect of Reaction Temperature

Ghamdi et al. reported the temperature effect on ODH experiments over partially reduced catalysts [12]. During successive injection ODH experiments, propylene selectivity showed a gradual increase with increasing reaction temperature. This is attributed to the variation of the catalyst degree

of reduction with both reaction temperature and the number of propane injections. At higher degrees of reduction of the catalysts, the ODH selective pathway is preferred over that for propane combustion. CO_x formation is low due to the lower availability of lattice oxygen. Rostom et al. also reported similar behavior [60].

Temperature increases beyond 650 °C may result in a significant reduction of propylene yield due to the higher influence of unselective thermal reactions [112]. Thus, thermal levels above 650 °C for PODH are not recommended. Furthermore, a certain extent of surface reduction occurs at temperatures below 650 °C, which is recommended for high propylene selectivity.

7.2. Effect of Reaction Time

Increasing reaction time augments propane conversion, enhances propylene selectivity, and decreases CO_x selectivity [12,60]. In this respect, longer contact times yield higher lattice oxygen utilization, favoring propylene formation and decreasing CO_x. However, very long reaction times are not favorable, as they may allow for the products (i.e., propylene) to re-adsorb on the catalyst surface, lowering propylene selectivity and increasing CO_x selectivity. Furthermore, long reaction times (more than 20 s) are not adequate for industrial use, given that they would require additional lengths of downflow fluidized beds to be included in the reactor system.

8. Reactor Concepts for PODH

Adsorption and desorption during PODH reactions are governed by phase residence times, chemical species interaction with each other, and with the catalyst. The reactor type and the operation mode, in turn, determine these factors. Efficient heat removal from the PODH process is a major concern for reactor operation, given that PODH is an exothermic reaction.

8.1. Fixed-Bed Reactors

Most of the ODH literature references consider fixed-bed type reactors, mainly due to their perceived operational simplicity [8,40,74,113–115]. For instance, temperature gradients can hardly be eliminated in a traditional fixed-bed reactor unless the catalyst bed is diluted with inert particles while using a large inert particle/catalyst particle ratio. This greatly increases the fixed cost and it is a significant challenge for the economical industrial scale production of propylene that is based on the PODH process.

Researchers analyzed multi-tubular reactors with periodic air injection [116], membrane reactors [117], and wall-cooled catalytic reactors [118] to overcome the exothermicity of ODH fixed-bed reactors. The aim was to efficiently remove the generated heat from the catalyst bed. A micro-channel reactor was utilized to reduce the fixed-bed reactor cost [21]. It is reported that the micro-channel reactor can achieve the same reactor productivity as a traditional fixed-bed reactor with less than 20% of the fixed-bed reactor volume. This is the case, given the inherent suitability of micro-channel reactors for highly exothermic reactions, due to their excellent heat transfer and heat removal capabilities.

Recently, the performances of phase-pure M1 $MoVNbTeO_x$ catalysts in the ODHE reaction in both a micro-channel reactor and a small-sized fixed-bed reactor, under same conditions, were investigated [21]. This comparison was carried out to demonstrate the advantages of the micro-channel reactors for improved heat management. XRD, SEM, and ICP characterization indicated that the M1-PVA catalyst plate has a high stability in the micro-channel system.

8.2. Twin Circulating Fluidized Bed Reactors for PODH

Circulating fluidized bed reactors and, more specifically downer reactors for ODH, have received much attention recently due to the several shortcomings of the fixed-bed reactors [3,60,102]. Downer reactors, if operated with fine particles in the 60–100 micron range, provide controlled thermal change, adequate particle concentration, and residence times, allowing an ODH with high olefin selectivity [67].

In ODH, under oxygen-free atmospheres and once the surface lattice oxygen has been exhausted, the rate of water formation decreases. This occurs with a gradual increase in the formation of molecular H_2, which, in turn, slows down the ODH reaction. Therefore, catalyst re-oxidation (regeneration) is necessary for adequate catalyst activity [45,61,96,116,119,120]. Thus, in ODH, periodic catalyst re-oxidations are required and, as a result, the ODH process can be viewed as a system of twin fluidized reactors: an oxidative dehydrogenation reactor and a re-oxidation reactor [12,59,61] (Figure 8). In these ODH systems, the gas phase oxygen is never allowed to reach the oxidative dehydrogenation unit. This limits the possibility of the complete combustion of the propane feed and propylene product.

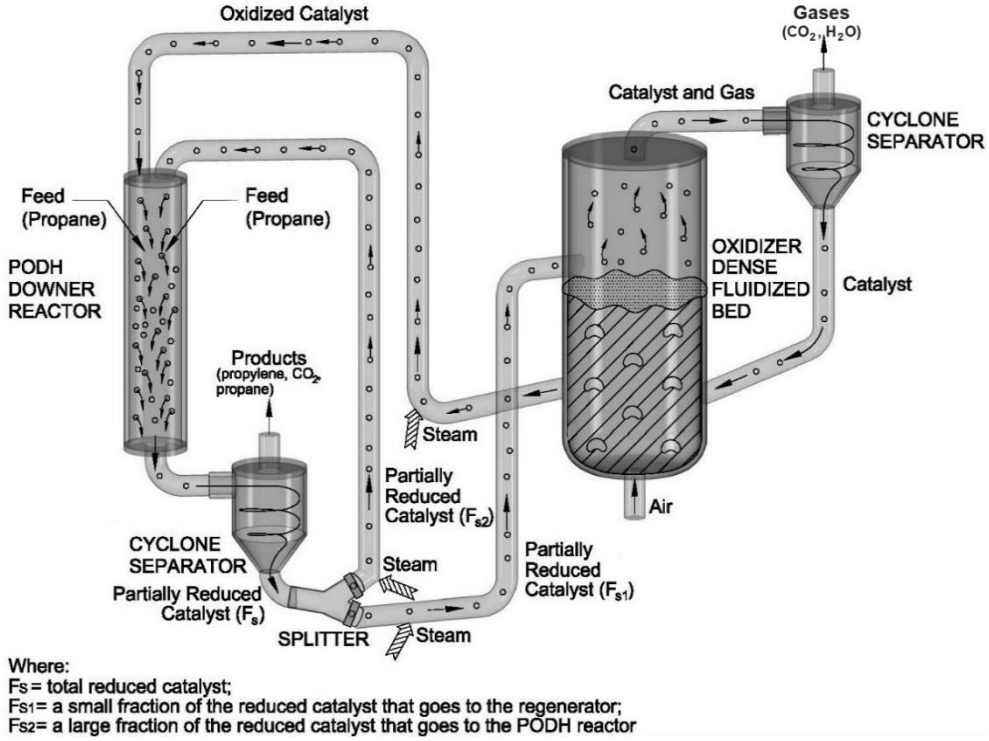

Figure 8. Schematic Oxidative Dehydrogenation (ODH) Process Flow Sheet Displaying the Anticipated Industrial Operation for a PODH Process. Adapted with permission from [59], copyright 2017, American Chemical Society.

Thus, a remaining outstanding challenge for ODH is to have available fluidizable catalysts with high selectivity towards propylene formation and be able to supply oxygen for dehydrogenation. Therefore, the most important characteristics of a successful ODH catalyst are its activity in the ODH reactor and its reactivity in the re-oxidation cycle. In addition, the fluidizable ODH catalysts should: (a) be stable under repeated reduction/oxidation cycles, (b) be resistant to agglomeration, (c) be able to withstand the friction stress that is associated with the high circulation of particles, and (d) be environmentally benign and affordable.

8.3. Circulating Fluidized Bed Reactor Models for PODH

The technical literature reports a mathematical model for PODH. The model was based on a two-phase fluidized bed reactor representation [68]. The model used the kinetics for a V-Mg oxide catalyst. Simulations showed that temperature, pressure, feed composition, particle size, and gas velocity were all factors affecting propane conversion and propylene selectivity. The model was validated while using previously published experimental data from a circulating fluidized bed reactor unit.

Recently, Rostom et al. [121] reported a downer fluidized bed reactor simulation using a hybrid CPFD Barracuda software, which represents the catalyst particles as particle clusters. The kinetics

established using experimental data were incorporated in the simulation. The data showed good propane conversion and propylene selectivity prospects for an industrial scale unit.

9. PODH Industrial Prospects

ODH under oxygen-free atmosphere, with the source of oxygen being the catalyst lattice oxygen, offers unique advantages. Catalyst lattice oxygen, instead of gas phase molecular oxygen or other mild oxidants, prevents deep alkane oxidation, thus limiting CO_x formation. This catalytic reaction leads to higher olefin selectivity, securing a much more energy efficient route for olefin production. To accomplish this, Rostom et al. [121] recently reported an industrial PODH process, where the PODH catalyst is circulated between a PODH reactor and a catalyst regenerator unit. After leaving the PODH reactor, the catalyst is divided in a splitter. Using this device, a major portion of the catalyst is recirculated back to the PODH reactor with a smaller fraction going to the regenerator (1/10 times) to be reactivated via re-oxidation. In this way, a partially reduced catalyst is always maintained, circulating in between the systems. This special reactor configuration helps to overcome the negative influence of combustion reactions, increasing as a result of overall propylene selectivity. It is envisioned that the industrial scale downer reactor for PODH will involve a 20 m length with 2.8–3.5 m/s particle cluster velocities and contact times in the 5–7 s range.

10. Conclusions

(a) The oxidative dehydrogenation of propane using vanadium-based catalysts offers valuable prospects for olefin production.

(b) In particular, vanadium-based catalysts supported on variety of fluidizable supports can be utilized to develop a suitable propane oxy-dehydrogenation process. These fluidizable catalysts can supply the lattice oxygen that is required for high olefin selectivity.

(c) A variety of reaction mechanisms and kinetic models can be considered for PODH. However, if one aims to develop a PODH leading to high propylene selectivity, special experimental devices, such as the CREC Riser Simulator, must be used.

(d) This approach provides kinetic models that will represent the PODH, under the conditions of successive propane injections, which are identified as being the most favorable for high propylene selectivity.

(e) An appropriate reactor selection for PODH is an important aspect to consider when establishing PODH at the commercial scale. In this respect, special reactor configurations involving downer reactors with partial catalyst re-oxidation are favored to achieve high propylene selectivities in a continuous process.

Author Contributions: Writing of the review manuscript draft, S.R.; Review and writing of manuscript, H.d.L. All authors have read and agreed to the published version of the manuscript.

Funding: This research was funded by the Natural Sciences and Engineering Research Council of Canada (NSERC) and the University of Western Ontario, through grants awarded to Hugo de Lasa.

Acknowledgments: We would like to gratefully thank Florencia de Lasa who assisted with the editing of this paper and the drafting of the graphical abstract of the present article.

Conflicts of Interest: The authors declare no conflict of interest.

Appendix A. —Oxygen (O–S) Conversion during Consecutive Runs with the 7.5 wt. % V/ZrO_2-γAl_2O_3 Catalyst

The calculation of surface oxygen (O–S) conversion taking place for the 7.5 wt. % V/ZrO_2-γAl_2O_3 catalyst was developed as follows:

(a) First, the amount of bounded oxygen on the catalyst (O–S), designated as $O_{min,TPR}$ or minimum O–S available for PODH was calculated. This was done using hydrogen TPR (Ramp 15 °C/min) with

$H_2 + O - S = H_2O + S$ being the only reaction taking place. Ten hydrogen consecutive TPRs were developed with a total of 51.955 cm^3 O_2/g or 0.00323 mols of O–S obtained.

(b) Furthermore, calculation of the same $O_{min,RS}$ or minimum oxygen(O–S) parameter in the CREC Riser Simulator was then calculated considering 0.76 g, the typical catalyst loading. This calculated $O_{min,RS}$ amounted in the CREC Riser Simulator to 0.00323 mol O–S.

(c) Finally and once $O_{min\text{-}RS}$ established, cumulative O–S consumption or O–S conversion via 10 consecutive propane injections in the CREC Riser Simulator was effected. This calculation accounted for a propane conversion per injection and the CO_2 and C_3H_6 selectivities from C_3H_8 + O–S → C_3H_6 + H_2O + S and C_3H_8 + 10 O–S → 3CO_2 + 4 H_2O + S reactions.

Application of this methodology showed a progressive increasing $O_{min,RS}$ conversion reaching in injection 10 a 72.9% value as shown in Figure A1. One should notice that under these conditions both high C_3H_6 and low CO_2 selectivity were observed and adequate O–S availability until the last tenth injection was shown.

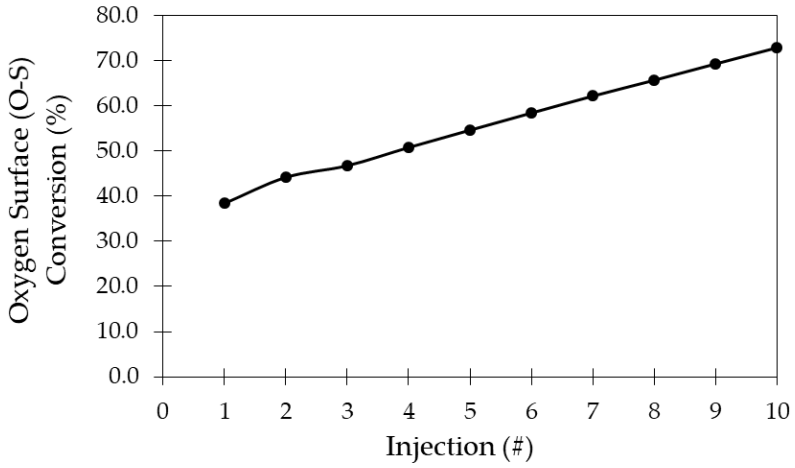

Figure A1. O–S Surface Oxygen Cumulative Conversion with the Propane Consecutive Injections for 7.5 wt. % V/ZrO_2-γAl_2O_3 catalyst at 550 °C in the CREC Riser Simulator.

References

1. Bai, P.T.; Manokaran, V.; Saiprasad, P.S.; Srinath, S. Studies on Heat and Mass Transfer Limitations in Oxidative Dehydrogenation of Ethane Over Cr_2O_3 /Al_2O_3 Catalyst. *Procedia Eng.* **2015**, *127*, 1338–1345. [CrossRef]
2. Khadzhiev, S.N.; Usachev, N.Y.; Gerzeliev, I.M.; Belanova, E.P.; Kalinin, V.P.; Kharlamov, V.V.; Kazakov, A.V.; Kanaev, S.A.; Starostina, T.S.; Popov, A.Y. Oxidative dehydrogenation of ethane to ethylene in a system with circulating microspherical metal oxide oxygen carrier: 1. Synthesis and study of the catalytic system. *Pet. Chem.* **2015**, *55*, 651–654. [CrossRef]
3. Bakare, I.A.; Mohamed, S.A.; Al-Ghamdi, S.; Razzak, S.A.; Hossain, M.M.; de Lasa, H.I. Fluidized bed ODH of ethane to ethylene over VO_x-MoO_x/γ-Al_2O_3 catalyst: Desorption kinetics and catalytic activity. *Chem. Eng. J.* **2015**, *278*, 207–216. [CrossRef]
4. Zhai, Z.; Wang, X.; Licht, R.; Bell, A.T. Selective oxidation and oxidative dehydrogenation of hydrocarbons on bismuth vanadium molybdenum oxide. *J. Catal.* **2015**, *325*, 87–100. [CrossRef]
5. H.Zea, L.C. Oxidative dehydrogenation of propane on Pd-Mo/gamma-Al_2O_3 catalyst: A kinetic study. *Aust. J. Basic Appl. Sci.* **2015**, *9*, 78–83.
6. Khalil, Y.P. Propylene in Demand: Roadblocks and Opportunities. 2015. Available online: https://insights.globalspec.com/article/473/propylene-in-demand-roadblocks-and-opportunities (accessed on 9 April 2020).
7. Rebsdat, S.; Mayer, D. Ethylene Glycol. *Ullmann's Encycl. Ind. Chem.* **2012**. [CrossRef]
8. Darvishi, A.; Davand, R.; Khorasheh, F.; Fattahi, M. Modeling-based optimization of a fixed-bed industrial reactor for oxidative dehydrogenation of propane. *Chin. J. Chem. Eng.* **2016**, *24*, 612–622. [CrossRef]

9. Elbadawi, A.H.; Osman, M.S.; Razzak, S.A.; Hossain, M.M. VO_x-Nb/La-γAl_2O_3 catalysts for oxidative dehydrogenation of ethane to ethylene. *J. Taiwan Inst. Chem. Eng.* **2016**, *61*, 106–116. [CrossRef]
10. Ayandiran, A.A.; Bakare, I.A.; Binous, H.; Al-Ghamdi, S.; Razzak, S.A.; Hossain, M.M. Oxidative dehydrogenation of propane to propylene over VO_x/CaO–γ-Al_2O_3 using lattice oxygen. *Catal. Sci. Technol.* **2016**, *6*, 5154–5167. [CrossRef]
11. Bhasin, M.M. Is true ethane oxydehydrogenation feasible? *Top. Catal.* **2003**, *23*, 145–149. [CrossRef]
12. Al-Ghamdi, S.A.; de Lasa, H.I. Propylene production via propane oxidative dehydrogenation over VO_x/γ-Al_2O_3 catalyst. *Fuel* **2014**, *128*, 120–140. [CrossRef]
13. Gao, Y.; Neal, L.M.; Li, F. Li-Promoted La_xSr_2-xFeO_4-δ Core—Shell Redox Catalysts for Oxidative Dehydrogenation of Ethane under a Cyclic Redox Scheme. *ACS Catal.* **2016**, *6*, 7293–7302. [CrossRef]
14. Setnička, M.; Tišler, Z.; Kubička, D.; Bulánek, R. Activity of Molybdenum Oxide Catalyst Supported on Al_2O_3, TiO_2, and SiO_2 Matrix in the Oxidative Dehydrogenation of n-Butane. *Top. Catal.* **2015**, *58*, 866–876. [CrossRef]
15. Koirala, R.; Buechel, R.; Pratsinis, S.E.; Baiker, A. Silica is preferred over various single and mixed oxides as support for CO_2-assisted cobalt-catalyzed oxidative dehydrogenation of ethane. *Appl. Catal. A Gen.* **2016**, *527*, 96–108. [CrossRef]
16. Ren, T.; Patel, M.; Blok, K. Olefins from conventional and heavy feedstocks: Energy use in steam cracking and alternative processes. *Energy* **2006**, *31*, 425–451. [CrossRef]
17. Barghi, B.; Fattahi, M.; Khorasheh, F. The Modeling of Kinetics and Catalyst Deactivation in Propane Dehydrogenation Over Pt-Sn/γ-Al_2O_3 in Presence of Water as an Oxygenated Additive. *Pet. Sci. Technol.* **2014**, *32*, 1139–1149. [CrossRef]
18. Cavani, F.; Trifirò, F. The oxidative dehydrogenation of ethane and propane as an alternative way for the production of light olefins. *Catal. Today* **1995**, *24*, 307–313. [CrossRef]
19. Sanfilippo, D. Dehydrogenation of Paraffins; Key Technology for Petrochemicals and Fuels. *Cattech* **2000**, *4*, 56–73. [CrossRef]
20. Cavani, F.; Ballarini, N.; Cericola, A. Oxidative dehydrogenation of ethane and propane: How far from commercial implementation? *Catal. Today* **2007**, *127*, 113–131. [CrossRef]
21. Chu, B.; Truter, L.; Nijhuis, T.A.; Cheng, Y. Oxidative dehydrogenation of ethane to ethylene over phase-pure M1 MoVNbTeO_x catalysts in a micro-channel reactor. *Catal. Sci. Technol.* **2015**, *5*, 2807–2813. [CrossRef]
22. Botková, Š.; Čapek, L.; Setnička, M.; Bulánek, R.; Čičmanec, P.; Kalužová, A.; Pastva, J.; Zukal, A. VO_x species supported on Al_2O_3-SBA-15 prepared by the grafting of alumina onto SBA-15: Structure and activity in the oxidative dehydrogenation of ethane. *React. Kinet Mech. Catal.* **2016**, *119*, 319–333. [CrossRef]
23. Koc, S.N.; Dayioglu, K.; Ozdemir, H. Oxidative dehydrogenation of propane with K-MoO_3/$MgAl_2O_4$ catalysts. *J. Chem. Sci.* **2016**, *128*, 67–71. [CrossRef]
24. Kong, L.; Li, J.; Zhao, Z.; Liu, Q.; Sun, Q.; Liu, J.; Wei, Y. Oxidative dehydrogenation of ethane to ethylene over Mo-incorporated mesoporous SBA-16 catalysts: The effect of MoO_x dispersion. *Appl. Catal. A Gen.* **2016**, *510*, 84–97. [CrossRef]
25. Jermy, B.R.; Ajayi, B.P.; Abussaud, B.A.; Asaoka, S.; Al-Khattaf, S. Oxidative dehydrogenation of n-butane to butadiene over Bi-Ni-O/γ-alumina catalyst. *J. Mol. Catal. A Chem.* **2015**, *400*, 121–131. [CrossRef]
26. Gascón, J.; Valenciano, R.; Téllez, C.; Herguido, J.; Menéndez, M. A generalized kinetic model for the partial oxidation of n-butane to maleic anhydride under aerobic and anaerobic conditions. *Chem. Eng. Sci.* **2006**, *61*, 6385–6394. [CrossRef]
27. Rubio, O.; Herguido, J.; Menéndez, M. Oxidative dehydrogenation of n-butane on V/MgO catalysts-kinetic study in anaerobic conditions. *Chem. Eng. Sci.* **2003**, *58*, 4619–4627. [CrossRef]
28. Wu, Y.; Gao, J.; He, Y.; Wu, T. Preparation and characterization of Ni-Zr-O nanoparticles and its catalytic behavior for ethane oxidative dehydrogenation. *Appl. Surf. Sci.* **2012**, *258*, 4922–4928. [CrossRef]
29. Fattahi, M.; Kazemeini, M.; Khorasheh, F.; Rashidi, A. An investigation of the oxidative dehydrogenation of propane kinetics over a vanadium-graphene catalyst aiming at minimizing of the CO_x species. *Chem. Eng. J.* **2014**, *250*, 14–24. [CrossRef]
30. Mukherjee, D.; Park, S.-E.; Reddy, B.M. CO_2 as a soft oxidant for oxidative dehydrogenation reaction: An eco benign process for industry. *J. CO2 Util.* **2016**, *16*, 301–312. [CrossRef]

31. Frank, B.; Dinse, A.; Ovsitser, O.; Kondratenko, E.V.; Schomäcker, R. Mass and heat transfer effects on the oxidative dehydrogenation of propane (ODP) over a low loaded VO_x/Al_2O_3 catalyst. *Appl. Catal. A Gen.* **2007**, *323*, 66–76. [CrossRef]
32. Valverde, J.A.; Echavarría, A.; Eon, J.-G.; Faro, A.C.; Palacio, L.A. V-Mg-Al catalyst from hydrotalcite for the oxidative dehydrogenation of propane. *React. Kinet. Mech. Catal.* **2014**, *111*, 679–696. [CrossRef]
33. Fukudome, K.; Suzuki, T. Highly Selective Oxidative Dehydrogenation of Propane to Propylene over VO_x-SiO_2 Catalysts. *Catal. Surv. Asia* **2015**, *19*, 172–187. [CrossRef]
34. Siahvashi, A.; Chesterfield, D.; Adesina, A.A. Nonoxidative and Oxidative Propane Dehydrogenation over Bimetallic Mo-Ni/Al_2O_3 Catalyst. *Ind. Eng. Chem. Res.* **2013**, *52*, 4017–4026. [CrossRef]
35. Sinev, M.Y.; Fattakhova, Z.T.; Tulenin, Y.P.; Stennikov, P.S.; Vislovskii, V.P. Hydrogen formation during dehydrogenation of C_2-C_4 alkanes in the presence of oxygen: Oxidative or non-oxidative? *Catal. Today* **2003**, *81*, 107–116. [CrossRef]
36. Fu, B.; Lu, J.; Stair, P.C.; Xiao, G.; Kung, M.C.; Kung, H.H. Oxidative dehydrogenation of ethane over alumina-supported Pd catalysts. Effect of alumina overlayer. *J. Catal.* **2013**, *297*, 289–295. [CrossRef]
37. Carrero, C.; Kauer, M.; Dinse, A.; Wolfram, T.; Hamilton, N.; Trunschke, A.; Schlögl, R.; Schomäcker, R. High performance $(VO_x)_n$-$(TiO_x)_m$/SBA-15 catalysts for the oxidative dehydrogenation of propane. *Catal. Sci. Technol.* **2014**, *4*, 786. [CrossRef]
38. Carrero, C.A.; Schlögl, R.; Wachs, I.E.; Schomaecker, R. Critical literature review of the kinetics for the oxidative dehydrogenation of propane over well-defined supported vanadium oxide catalysts. *ACS Catal.* **2014**, *4*, 3357–3380. [CrossRef]
39. Dar, H.J.; Nanot, S.U.; Jens, K.J.; Jakobsen, H.A.; Tangstad, E.; Chen, D. Kinetic Analysis and Upper Bound of Ethylene Yield of Gas Phase Oxidative Dehydrogenation of Ethane to Ethylene. *Ind. Eng. Chem. Res.* **2012**, *51*, 10571–10585. [CrossRef]
40. Ahmed, S.; Rahman, F.; Al-Amer, A.M.J.; Al-Mutairi, E.M.; Baduruthamal, U.; Alam, K. Oxidative dehydrogenation of lower alkanes over metal incorporated MCM-41 catalysts. *React. Kinet. Mech. Catal.* **2012**, *105*, 483–493. [CrossRef]
41. Schwarz, O.; Habel, D.; Ovsitser, O.; Kondratenko, E.V.; Hess, C.; Schomäcker, R.; Schubert, H. Impact of preparation method on physico-chemical and catalytic properties of VO_x/γ-Al_2O_3 materials. *J. Mol. Catal. A Chem.* **2008**, *293*, 45–52. [CrossRef]
42. Mishanin, I.I.; Kalenchuk, A.N.; Maslakov, K.I.; Lunin, V.V.; Koklin, A.E.; Finashina, E.D.; Bogdan, V.I. Deactivation of a mixed oxide catalyst of Mo-V-Te-Nb-O composition in the reaction of oxidative ethane dehydrogenation. *Russ. J. Phys. Chem. A* **2016**, *90*, 1132–1136. [CrossRef]
43. Ajayi, B.P.; Rabindran Jermy, B.; Abussaud, B.A.; Al-Khattaf, S. Oxidative dehydrogenation of n-butane over bimetallic mesoporous and microporous zeolites with CO_2 as mild oxidant. *J. Porous Mater.* **2013**, *20*, 1257–1270. [CrossRef]
44. Koirala, R.; Buechel, R.; Krumeich, F.; Pratsinis, S.E.; Baiker, A. Oxidative Dehydrogenation of Ethane with CO_2 over Flame-Made Ga-Loaded TiO_2. *ACS Catal.* **2015**, *5*, 690–702. [CrossRef]
45. Kowalska-Kuś, J.; Held, A.; Nowińska, K. Oxydehydrogenation of C_2-C_4 hydrocarbons over Fe-ZSM-5 zeolites with N_2O as an oxidant. *Catal. Sci. Technol.* **2013**, *3*, 508–518. [CrossRef]
46. Kondratenko, E.V.; Cherian, M.; Baerns, M.; Su, D.; Schlogl, R.; Wang, X.; Wachs, I.E. Oxidative dehydrogenation of propane over V/MCM-41 catalysts: Comparison of O_2 and N_2O as oxidants. *J. Catal.* **2005**, *234*, 131–142. [CrossRef]
47. Védrine, J. Heterogeneous Partial (amm) Oxidation and Oxidative Dehydrogenation Catalysis on Mixed Metal Oxides. *Catalysts* **2016**, *6*, 22. [CrossRef]
48. Talati, A.; Haghighi, M.; Rahmani, F. Impregnation vs. coprecipitation dispersion of Cr over TiO_2 and ZrO_2 used as active and stable nanocatalysts in oxidative dehydrogenation of ethane to ethylene by carbon dioxide. *RSC Adv.* **2016**, *6*, 44195–44204. [CrossRef]
49. Liu, H.; Zhang, Z.; Li, H.; Huang, Q. Intrinsic kinetics of oxidative dehydrogenation of propane in the presence of CO_2 over Cr/MSU-1 catalyst. *J. Nat. Gas Chem.* **2011**, *20*, 311–317. [CrossRef]
50. Qiao, A.; Kalevaru, V.N.; Radnik, J.; Martin, A. Oxidative dehydrogenation of ethane to ethylene over Ni-Nb-M-O catalysts: Effect of promoter metal and CO_2-admixture on the performance. *Catal. Today* **2016**, *264*, 144–151. [CrossRef]

51. Elfadly, A.M.; Badawi, A.M.; Yehia, F.Z.; Mohamed, Y.A.; Betiha, M.A.; Rabie, A.M. Selective nano alumina supported vanadium oxide catalysts for oxidative dehydrogenation of ethylbenzene to styrene using CO_2 as soft oxidant. *Egypt. J. Pet.* **2013**, *22*, 373–380. [CrossRef]
52. Ramesh, Y.; Thirumala Bai, P.; Hari Babu, B.; Lingaiah, N.; Rama Rao, K.S.; Prasad, P.S.S. Oxidative dehydrogenation of ethane to ethylene on Cr_2O_3/Al_2O_3-ZrO_2 catalysts: The influence of oxidizing agent on ethylene selectivity. *Appl. Petrochem. Res.* **2014**, *4*, 247–252. [CrossRef]
53. Raju, G.; Reddy, B.M.; Abhishek, B.; Mo, Y.; Park, S. Synthesis of C_4 olefins from n-butane over a novel VO_x/SnO_2-ZrO_2 catalyst using CO_2 as soft oxidant. *Appl. Catal. A Gen.* **2012**, *423–424*, 168–175. [CrossRef]
54. Elbadawi, A.H.; Ba-Shammakh, M.S.; Al-Ghamdi, S.; Razzak, S.A.; Hossain, M.M.; de Lasa, H.I. Phenomenologically based kinetics of ODH of ethane to ethylene using lattice oxygen of VO_x/Al_2O_3-ZrO_2 catalyst. *Chem. Eng. Res. Des.* **2017**, *117*, 733–745. [CrossRef]
55. Al-Ghamdi, S.; Volpe, M.; Hossain, M.M.; de Lasa, H. VO_x/c-Al_2O_3 catalyst for oxidative dehydrogenation of ethane to ethylene: Desorption kinetics and catalytic activity. *Appl. Catal. A Gen.* **2013**, *450*, 120–130. [CrossRef]
56. Elbadawi, A.H.; Ba-Shammakh, M.S.; Al-Ghamdi, S.; Razzak, S.A.; Hossain, M.M.; de Lasa, H.I. A fluidizable VO_x/γ-Al_2O_3-ZrO_2 catalyst for the ODH of ethane to ethylene operating in a gas phase oxygen free environment. *Chem. Eng. Sci.* **2016**, *145*, 59–70. [CrossRef]
57. Sedor, K.E.; Hossain, M.M.; De Lasa, H.I. Reduction kinetics of a fluidizable nickel-alumina oxygen carrier for chemical-looping combustion. *Can. J. Chem. Eng.* **2008**, *86*, 323–334. [CrossRef]
58. Khan, M.Y.; Al-Ghamdi, S.; Razzak, S.A.; Hossain, M.M.; de Lasa, H. Fluidized bed oxidative dehydrogenation of ethane to ethylene over VO_x/Ce-γAl_2O_3catalysts: Reduction kinetics and catalyst activity. *Mol. Catal.* **2017**, *443*, 78–91. [CrossRef]
59. Rostom, S.; de Lasa, H.I. Propane Oxidative Dehydrogenation Using Consecutive Feed Injections and Fluidizable $VO_x/\gamma Al_2O_3$ and VO_x/ZrO_2-γAl_2O_3 Catalysts. *Ind. Eng. Chem. Res.* **2017**, *56*, 13109–13124. [CrossRef]
60. Rostom, S.; Lasa, H. De High Propylene Selectivity via Propane Oxidative Dehydrogenation Using a Novel Fluidizable Catalyst: Kinetic Modeling. *Ind. Eng. Chem. Res.* **2018**, *57*, 10251–10260. [CrossRef]
61. Hossain, M.M. Kinetics of Oxidative Dehydrogenation of Propane to Propylene Using Lattice Oxygen of VO_x/CaO/γAl_2O_3 Catalysts. *Ind. Eng. Chem. Res.* **2017**, *56*, 4309–4318. [CrossRef]
62. Fukudome, K.; Ikenaga, N.O.; Miyake, T.; Suzuki, T. Oxidative dehydrogenation of alkanes over vanadium oxide prepared with $V(t\text{-}BuO)_3O$ and $Si(OEt)_4$ in the presence of polyethyleneglycol. *Catal. Today* **2013**, *203*, 10–16. [CrossRef]
63. Fukudome, K.; Ikenaga, N.; Miyake, T.; Suzuki, T. Oxidative dehydrogenation of propane using lattice oxygen of vanadium oxides on silica. *Catal. Sci. Technol.* **2011**, *1*, 987. [CrossRef]
64. Rischard, J.; Antinori, C.; Maier, L.; Deutschmann, O. Oxidative dehydrogenation of n-butane to butadiene with Mo-V-MgO catalysts in a two-zone fluidized bed reactor. *Appl. Catal. A Gen.* **2016**, *511*, 23–30. [CrossRef]
65. Rodríguez, M.L.; Ardissone, D.E.; López, E.; Pedernera, M.N.; Borio, D.O. Reactor designs for ethylene production via ethane ODH: Comparison of performance. *Engineering* **2010**, *2010*, 45–46.
66. Chalakov, L.; Rihko-Struckmann, L.K.; Munder, B.; Sundmacher, K. Oxidative dehydrogenation of ethane in an electrochemical packed-bed membrane reactor: Model and experimental validation. *Chem. Eng. J.* **2009**, *145*, 385–392. [CrossRef]
67. Zaynali, Y.; Alavi-Amleshi, S.M. Comparative study of propane oxidative dehydrogenation in fluidized and fixed bed reactor. *Part. Sci. Technol.* **2016**, *6351*, 1–7. [CrossRef]
68. Torabi, A.; Kazemeini, M.; Fattahi, M. Developing a mathematical model for the oxidative dehydrogenation of propane in a fluidized bed reactor. *Asia-Pac. J. Chem. Eng.* **2016**, *11*, 448–459. [CrossRef]
69. Smith, J.M.; Van Ness, H.C.; Abbott, M.M. *Introduction to Chemical Engineering Thermodynamics*; McGraw-Hill Education: New York, NY, USA, 2005; Volume 27.
70. Hossain, M.M. Chemical-Looping Combustion with Gaseous Fuels: Thermodynamic Parametric Modeling. *Arab. J. Sci. Eng.* **2014**, *39*, 3415–3421. [CrossRef]
71. De Lasa, H.; Salaices, E.; Mazumder, J.; Lucky, R. Catalytic steam gasification of biomass: Catalysts, thermodynamics and kinetics. *Chem. Rev.* **2011**, *111*, 5404–5433. [CrossRef]
72. Grant, J.T.; Love, A.M.; Carrero, C.A.; Huang, F.; Panger, J.; Verel, R.; Hermans, I. Improved Supported Metal Oxides for the Oxidative Dehydrogenation of Propane. *Top. Catal.* **2016**, *59*, 1545–1553. [CrossRef]

73. Zea, H.; Carballo, L.M. Kinetic evaluation of Pd alumina supported catalyst for the reaction of oxidative dehydrogenation of propane. *ARPN J. Eng. Appl. Sci.* **2015**, *10*, 896–900.
74. Qiao, A.; Kalevaru, V.N.; Radnik, J.; Düvel, A.; Heitjans, P.; Kumar, A.S.H.; Prasad, P.S.S.; Lingaiah, N.; Martin, A. Oxidative Dehydrogenation of Ethane to Ethylene over V_2O_5/Al_2O_3 Catalysts: Effect of Source of Alumina on the Catalytic Performance. *Ind. Eng. Chem. Res.* **2014**, *53*, 18711–18721. [CrossRef]
75. Elbadawi, A.H.; Ba-Shammakh, M.S.; Al-Ghamdi, S.; Razzak, S.A.; Hossain, M.M. Reduction kinetics and catalytic activity of VO_x/γ-Al_2O_3-ZrO_2 for gas phase oxygen free ODH of ethane. *Chem. Eng. J.* **2016**, *284*, 448–457. [CrossRef]
76. Zaynali, Y.; Alavi, S. Higher propene yield by tailoring operating conditions of propane oxidative dehydrogenation over V_2O_5/γ-Al_2O_3. *J. Serb. Chem. Soc.* **2015**, *80*, 355–366. [CrossRef]
77. Fattahi, M.; Kazemeini, M.; Khorasheh, F.; Rashidi, A.M. Vanadium Pentoxide Catalyst over Carbon-Based Nanomaterials for the Oxidative Dehydrogenation of Propane. *Ind. Eng. Chem. Res.* **2013**, *52*, 16128–16141. [CrossRef]
78. Kazemeini, M. Physicochemical Properties and Catalytic Performances of Nanostructured V_2O_5 over TiO_2 and γ-Al_2O_3 for Oxidative Dehydrogenation of Propane. *Chem. Biochem. Eng. Q. J.* **2016**, *30*, 9–18. [CrossRef]
79. Oyama, S.T.; Somorjai, G.A. Effect of structure in selective oxide catalysis: Oxidation reactions of ethanol and ethane on vanadium oxide. *J. Phys. Chem.* **1990**, *94*, 5022–5028. [CrossRef]
80. Ciambelli, P.; Galli, P.; Lisi, L.; Massucci, M.A.; Patrono, P.; Pirone, R.; Ruoppolo, G.; Russo, G. TiO_2 supported vanadyl phosphate as catalyst for oxidative dehydrogenation of ethane to ethylene. *Appl. Catal. A Gen.* **2000**, *203*, 133–142. [CrossRef]
81. Dinse, A.; Schomäcker, R.; Bell, A.T. The role of lattice oxygen in the oxidative dehydrogenation of ethane on alumina-supported vanadium oxide. *Phys. Chem. Chem. Phys.* **2009**, *11*, 6119. [CrossRef]
82. Xu, B.; Zhu, X.; Cao, Z.; Yang, L.; Yang, W. Catalytic oxidative dehydrogenation of n-butane over V_2O_5/MO-Al_2O_3 (M = Mg, Ca, Sr, Ba) catalysts. *Chin. J. Catal.* **2015**, *36*, 1060–1067. [CrossRef]
83. Martínez-Huerta, M.V.; Gao, X.; Tian, H.; Wachs, I.E.; Fierro, J.L.G.; Bañares, M.A. Oxidative dehydrogenation of ethane to ethylene over alumina-supported vanadium oxide catalysts: Relationship between molecular structures and chemical reactivity. *Catal. Today* **2006**, *118*, 279–287. [CrossRef]
84. Enache, D.I.; Bordes-Richard, E.; Ensuque, A.; Bozon-Verduraz, F. Vanadium oxide catalysts supported on zirconia and titania I. Preparation and characterization. *Appl. Catal. A Gen.* **2004**, *278*, 93–102.
85. Gao, X. In Situ UV-vis-NIR Diffuse Reflectance and Raman Spectroscopic Studies of Propane Oxidation over ZrO_2-Supported Vanadium Oxide Catalysts. *J. Catal.* **2002**, *209*, 43–50. [CrossRef]
86. Rossetti, I.; Mancini, G.F.; Ghigna, P.; Scavini, M.; Piumetti, M.; Bonelli, B.; Cavani, F.; Comite, A. Spectroscopic enlightening of the local structure of VO_x active sites in catalysts for the ODH of propane. *J. Phys. Chem. C* **2012**, *116*, 22386–22398. [CrossRef]
87. Weckhuysen, B.M.; Keller, D.E. Chemistry, spectroscopy and the role of supported vanadium oxides in heterogeneous catalysis. *Catal. Today* **2003**, *78*, 25–46. [CrossRef]
88. Wu, Z.; Kim, H.S.; Stair, P.C.; Rugmini, S.; Jackson, S.D. On the structure of vanadium oxide supported on aluminas: UV and visible Raman spectroscopy, UV-visible diffuse reflectance spectroscopy, and temperature-programmed reduction studies. *J. Phys. Chem. B* **2005**, *109*, 2793–2800. [CrossRef]
89. Argyle, M.D.; Chen, K.; Bell, A.T.; Iglesia, E. Effect of catalyst structure on oxidative dehydrogenation of ethane and propane on alumina-supported vanadia. *J. Catal.* **2002**, *208*, 139–149. [CrossRef]
90. Klose, F.; Wolff, T.; Lorenz, H.; Seidelmorgenstern, A.; Suchorski, Y.; Piorkowska, M.; Weiss, H. Active species on γ-alumina-supported vanadia catalysts: Nature and reducibility. *J. Catal.* **2007**, *247*, 176–193. [CrossRef]
91. Murgia, V.; Sham, E.; Gottifredi, J.C.; Torres, E.M.F. Oxidative dehydrogenation of propane and n-butane over alumina supported vanadium catalysts. *Lat. Am. Appl. Res.* **2004**, *34*, 75–82.
92. Wachs, I.E.; Jehng, J.-M.; Deo, G.; Weckhuysen, B.M.; Guliants, V.V.; Benziger, J.B. In situ Raman spectroscopy studies of bulk and surface metal oxide phases during oxidation reactions. *Catal. Today* **1996**, *32*, 47–55. [CrossRef]
93. Wachs, I.E.; Weckhuysen, B.M. Structure and reactivity of surface vanadium oxide species on oxide supports. *Appl. Catal. A Gen.* **1997**, *157*, 67–90. [CrossRef]
94. Deo, G.; Wachs, I.E. Reactivity of Supported Vanadium Oxide Catalysts: The Partial Oxidation of Methanol. *J. Catal.* **1994**, *146*, 323–334. [CrossRef]

95. Blasco, T.; Nieto, J.M.L.; Dejoz, A.; Vázquez, M.I. Influence of the acid-base character of supported vanadium catalysts on their catalytic properties for the oxidative dehydrogenation of n-butane. *J. Catal.* **1995**, *157*, 271–282. [CrossRef]
96. Nieto, J.L. The selective oxidative activation of light alkanes. From supported vanadia to multicomponent bulk V-containing catalysts. *Top. Catal.* **2006**, *41*, 3–15. [CrossRef]
97. Blasco, T.; Lopez-Nieto, J.M. Oxidative dyhydrogenation of short chain alkanes on supported vanadium oxide catalysts. *Appl. Catal. A Gen.* **1997**, *157*, 117–142. [CrossRef]
98. Galli, A.; López Nieto, J.M.; Dejoz, A.; Vazquez, M.I. The effect of potassium on the selective oxidation of n-butane and ethane over Al_2O_3-supported vanadia catalysts. *Catal. Lett.* **1995**, *34*, 51–58. [CrossRef]
99. Chen, K.; Bell, A.T.; Iglesia, E. The Relationship between the Electronic and Redox Properties of Dispersed Metal Oxides and Their Turnover Rates in Oxidative Dehydrogenation Reactions. *J. Catal.* **2002**, *209*, 35–42. [CrossRef]
100. Lemonidou, A.A.; Nalbandian, L.; Vasalos, I.A. Oxidative Dehydrogenation of Propane over Vanadium Oxide Based Catalysts: Effect of Support and Alkali Promoter. *Catal. Today* **2000**, *61*, 333–341. [CrossRef]
101. Al-Ghamdi, S.; Moreira, J.; de Lasa, H. Kinetic Modeling of Propane Oxidative Dehydrogenation over VO_x/γ-Al_2 O_3 Catalysts in the Chemical Reactor Engineering Center Riser Reactor Simulator. *Ind. Eng. Chem. Res.* **2014**, *53*, 15317–15332. [CrossRef]
102. Al-Ghamdi, S.A.; Hossain, M.M.; de Lasa, H.I. Kinetic Modeling of Ethane Oxidative Dehydrogenation over VO_x/Al_2O_3 Catalyst in a Fluidized-Bed Riser Simulator. *Ind. Eng. Chem. Res.* **2013**, *52*, 5235–5244. [CrossRef]
103. De Lasa, H.I. Riser Simulator. U.S. Patent 5,102,628, 7 April 1992.
104. De Lasa, H. Reactor and Multifunctional Riser and Downer Simulator. U.S. Patent 10,220,363, 5 March 2019.
105. Baerns, M.; Buyevskaya, O.V. Simple Chemical Processes Based on Low Molecular-Mass Alkanes as Chemical Feedstocks. *Catal. Today* **1998**, *45*, 13–22. [CrossRef]
106. Dinse, A.; Frank, B.; Hess, C.; Habel, D.; Schomäcker, R. Oxidative dehydrogenation of propane over low-loaded vanadia catalysts: Impact of the support material on kinetics and selectivity. *J. Mol. Catal. A Chem.* **2008**, *289*, 28–37. [CrossRef]
107. Daniell, W.; Ponchel, A.; Kuba, S.; Anderle, F.; Weingand, T.; Gregory, D.H.; Kno, H. Characterization and catalytic behavior of VO_x-CeO_2 catalysts for the oxidative dehydrogenation of propane. *Top. Catal.* **2002**, *20*, 65–74. [CrossRef]
108. Yang, S.; Iglesia, E.; Bell, A.T. Oxidative dehydrogenation of propane over $V_2O_5/MoO_3/Al_2O_3$ and $V_2O_5/Cr_2O_3/Al_2O_3$: Structural characterization and catalytic function. *J. Phys. Chem. B* **2005**, *109*, 8987–9000. [CrossRef]
109. Grabowski, R.; Słoczyński, J. Kinetics of oxidative dehydrogenation of propane and ethane on VO_x/SiO_2 pure and with potassium additive. *Chem. Eng. Process. Process Intensif.* **2005**, *44*, 1082–1093. [CrossRef]
110. Chen, K.; Iglesia, E.; Bell, A.T. Kinetic isotopic effects in oxidative dehydrogenation of propane on vanadium oxide catalysts. *J. Catal.* **2000**, *192*, 197–203. [CrossRef]
111. Balcaen, V.; Sack, I.; Olea, M.; Marin, G.B. Transient kinetic modeling of the oxidative dehydrogenation of propane over a vanadia-based catalyst in the absence of O_2. *Appl. Catal. A Gen.* **2009**, *371*, 31–42. [CrossRef]
112. Farjoo, A.; Khorasheh, F.; Niknaddaf, S.; Soltani, M. Kinetic modeling of side reactions in propane dehydrogenation over Pt-Sn/γ-Al_2O_3 catalyst. *Sci. Iran.* **2011**, *18*, 458–464. [CrossRef]
113. Fattahi, M.; Kazemeini, M.; Khorasheh, F.; Rashidi, A. Kinetic modeling of oxidative dehydrogenation of propane (ODHP) over a vanadium–graphene catalyst: Application of the DOE and ANN methodologies. *J. Ind. Eng. Chem.* **2014**, *20*, 2236–2247. [CrossRef]
114. You, R.; Zhang, X.; Luo, L.; Pan, Y.; Pan, H.; Yang, J.; Wu, L.; Zheng, X.; Jin, Y.; Huang, W. NbO_x/CeO_2-rods catalysts for oxidative dehydrogenation of propane: Nb-CeO_2 interaction and reaction mechanism. *J. Catal.* **2017**, *348*, 189–199. [CrossRef]
115. Wang, L.; Chu, W.; Jiang, C.; Liu, Y.; Wen, J.; Xie, Z. Oxidative dehydrogenation of propane over Ni-Mo-Mg-O catalysts. *J. Nat. Gas Chem.* **2012**, *21*, 43–48. [CrossRef]
116. Fattahi, M.; Kazemeini, M.; Khorasheh, F.; Darvishi, A.; Rashidi, A.M. Fixed-bed multi-tubular reactors for oxidative dehydrogenation in ethylene process. *Chem. Eng. Technol.* **2013**, *36*, 1691–1700. [CrossRef]
117. Kotanjac, Ž.S.; van Sint Annaland, M.; Kuipers, J.A.M. A packed bed membrane reactor for the oxidative dehydrogenation of propane on a Ga_2O_3/MoO_3 based catalyst. *Chem. Eng. Sci.* **2010**, *65*, 441–445. [CrossRef]

118. Che-Galicia, G.; Ruiz-Martínez, R.S.; López-Isunza, F.; Castillo-Araiza, C.O. Modeling of oxidative dehydrogenation of ethane to ethylene on a MoVTeNbO/TiO_2 catalyst in an industrial-scale packed bed catalytic reactor. *Chem. Eng. J.* **2015**, *280*, 682–694. [CrossRef]
119. Elbadawi, A.H.; Khan, M.Y.; Quddus, M.R.; Razzak, S.A.; Hossain, M.M. Kinetics of oxidative cracking of n-hexane to olefins over VO_x/Ce-Al_2O_3 under gas phase oxygen-free environment. *AIChE J.* **2017**, *63*, 130–138. [CrossRef]
120. Argyle, M.; Bartholomew, C. Heterogeneous Catalyst Deactivation and Regeneration: A Review. *Catalysts* **2015**, *5*, 145–269. [CrossRef]
121. Rostom, S.; Lasa, H. De Chemical Engineering & Processing: Process Intensification Downer fluidized bed reactor modeling for catalytic propane oxidative dehydrogenation with high propylene selectivity. *Chem. Eng. Process. Process Intensif.* **2019**, *137*, 87–99.